the MSG-AOM mice) and physiological saline (0.1 ml/10 g body wt, the MSG-Saline mice), respectively. Similarly, two groups of the ICR-Saline mice were given AOM or saline, belonging to groups 3 (11 males, the Saline-AOM mice) and 4 (5 males, the Saline–Saline). At the termination of the experiment (10 weeks after the last injection of AOM and 17 weeks of age of mice), all animals were killed to analyze the number of colonic ACF and BCAC, clinical serum chemistry and mRNA expression of IGF1, IGF2 and IGF-1R in the colonic mucosa.

Counting the numbers of ACF and BCAC

The ACF and BCAC were determined according to the standard procedures described previously (30,31,41). ACF are defined as single or multiple crypts that have altered luminal openings, exhibit thickened epithelia and are larger than adjacent normal crypts (35). BCAC, which have high-frequency mutations in β-*catenin* gene, demonstrate histological dysplasia with a disruption of the cellular morphology (Figure 2A) and an accumulation of this protein (Figure 2B) (39). BCAC do not have a typical ACF-like appearance because the lesion is not recognized on the mucosal surface like ACF and is only identified in the histological sections of 'en face' preparations. Both of these lesions are utilized as biomarkers to evaluate a number of agents for their potential chemopreventive (42–44) and tumor promotion (45) properties. After the colons were fixed flat in 10% buffered formalin for 24 h, the mucosal surface of the colons were stained with methylene blue (0.5% in distilled water) and then the number of ACF were counted under a light microscope. Thereafter, the distal parts (5 cm from anus) of the colon were cut to count the number of BCAC. To identify BCAC intramucosal lesions, the distal part of the colon (mean area: 0.7 cm^2/colon) was embedded in paraffin and then a total of 20 serial sections (4 μm thick each) per colon were made by an en face preparation (30,31,41). For each case, two serial sections were used to analyze BCAC.

Histopathology and immunohistochemical analyses for β-catenin and IGF-1R

Three serial sections were made from paraffin-embedded tissue blocks. Two sections were subjected to hematoxylin and eosin (H and E) staining for histopathology and β-catenin immunohistochemistry to count the number of BCAC. Immunohistochemistry for β-catenin and IGF-1R was performed using the labeled streptavidin-biotin method (LSAB kit; DAKO, Glostrup, Denmark), as described previously (30,31). Primary antibodies of anti-β-catenin antibody (1:1000 final dilution) and anti-IGF-1R antibody (1:100 final dilution) obtained from Transduction Laboratories (catalog no. 610154; San Jose, CA) and Santa Cruz Biotechnology, Inc. (sc-7907; Santa Cruz, CA), respectively, were applied on the sections. Negative control sections were immunostained without the primary antibody.

Blood chemistry

At 17 weeks of age, blood samples (0.5–1.0 ml/mouse) were collected for determination of total cholesterol, triglyceride and glucose by a simple measurement device (DRICHEM Fujifilm Medical Co., Ltd, Tokyo). The concentration of blood insulin was measured by an LBIS insulin measuring kit for mice (Shibayagi Co., Ltd, Gunma).

RNA extraction and quantitative real-time reverse transcription–polymerase chain reaction analysis

A quantitative real-time reverse transcription–polymerase chain reaction analysis was carried out in the scraped colonic mucosa of the MSG-AOM mice and the Salin-AOM mice. Total RNA was isolated from the scraped colon mucosa of the mice using the RNAqueous-4PCR kit (Ambion Applied Biosystems, Austin, TX). The cDNA was synthesized from 0.2 μg total RNA using the SuperScript III First-Strand Synthesis System (Invitrogen, Carlsbad, CA). The primers used for the amplification of IGF-1-, IGF-2- and IGF-1R-specific genes were as follows: IGF-1 forward, 5′-CTGGACCAGAGACCCTTTGC-3′ and reverse, 5′-GGACGGGGACTTCTGAGTCTT-3′; IGF-2 forward, 5′-GTGCTGCATCGCTGCTTAC-3′ and reverse, 5′-ACGTCCCTCTCGGACTTGG-3′; and IGF-1R forward, 5′-GTGGGGGCTCGTGTTTCTC-3′ and reverse, 5′-GATCACCGTGCAGTTTTCCA-3′. Real-time PCR was done in a LightCycler (Roche Diagnostics Co., Indianapolis, IN) with SYBR Premix Ex Taq (TaKaRa Bio, Shiga, Japan). The expression levels of the IGF-1, IGF-2 and IGF-1R genes were normalized to the β-actin gene expression level.

Statistical analysis

Measurements are expressed as mean ± SD, and differences if present were compared by one-way analysis of analysis of variance (Tukey–Kramer's multiple comparison's test) or two-tailed unpaired *t*-test. The incidences of intestinal tumors were compared by Fisher's exact probability test. The results were considered statistically significant if the *P* values were <0.05.

Results

General observations

As shown in Figure 1, the mean body weight of MSG–Saline mice (group 2) was much greater than Saline–Saline mice (group 4) during the study. The average body weights of the AOM-injected groups belonging to groups 1 (MSG-AOM) and 3 (Saline-AOM) were smaller than that of saline-injected groups, groups 2 (MSG-Saline) and 4 (Saline–Saline), during the study. At the termination of the experiment, the mean body weights of groups 1 and 3 were significantly lower than groups 2 and 4, respectively ($P < 0.001$), as listed in Table I.

The numbers of ACF and BCAC

ACF and BCAC (Figure 2A and B) developed in all the mice belonging to group 1 (the MSG-AOM mice) and 3 (the Saline-AOM mice) but not in the mice of groups 2 (the MSG-Saline) and 4 (the Saline-Salin mice) that did not receive AOM. Table I summarizes the total numbers of ACF and BCAC in all groups. The number of BCAC of group 1 was significantly greater than group 3 ($P < 0.001$), whereas the numbers of ACF developed in groups 1 and 3 were comparable.

Serum levels of glucose, total cholesterol, triglyceride and insulin

The serum concentrations of glucose, total cholesterol, triglyceride and insulin at 17 weeks of age are shown in Table II. MSG treatment significantly elevated all measures regardless of the AOM exposure (group 1 versus group 3, $P < 0.001$; and group 2 versus group 4, $P < 0.001$). However, the AOM administration did not affect all the measurements (group 1 versus group 2; and group 3 versus group 4).

β-Catenin and IGF-IR immunohistochemistry

Immunohistochemical expression of β-catenin revealed the presence of BCACs, where β-catenin was accumulated in the nucleus and/or cytoplasm (Figure 2B). Immunohistochemical expression of IGF-IR in the cytoplasm of BCAC that develop in the MSG-AOM mice was intensive when compared with the surrounding crypts (Figure 2C). Inflammatory cells infiltrated into the surrounding stroma of BCAC also showed positive reaction against IGF-1R.

mRNA expression levels of IGF-1, IGF-2 and IGF-1R in the colonic mucosa

The expression levels of IGF-1, IGF-2 and IGF-1R mRNAs of the colonic mucosa from the MSG-AOM mice (group 1) and the Saline-AOM mice (group 3) were determined. As illustrated in Figure 3, the MSG + AOM treatment mice showed significantly increased mRNA levels of IGF-1 (1. 81-fold increase) and IRF-1R (2.43-fold increase), when compared with the Saline-AOM mice. The increase of IGF-1R was statistically significant ($P < 0.01$). mRNA levels of IGF-2 of the two groups were comparable.

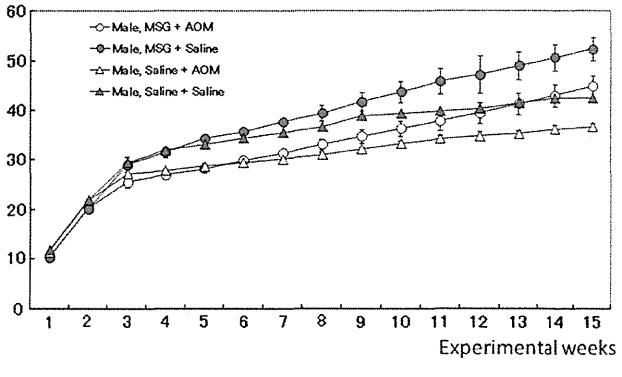

Fig. 1. Body weight gains of all groups during the study.

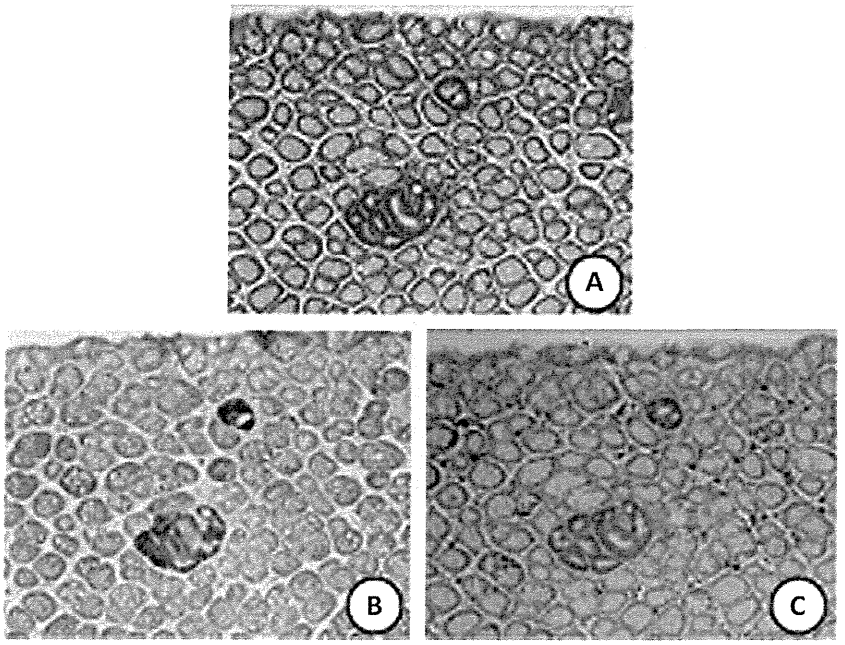

Fig. 2. Histopathology (**A**) of a BCAC developed in an MSG-AOM mouse. Immunohistochemistry of (**B**) β-catenin and (**C**) IGF-1R in the BCAC shows positive reaction of β-catenin in their cell membrane and cytoplasm and IGF-1R in their cytoplasm. Bars = 50 μm. (A) H and E stain, (B) β-catenin immunohistochemistry and (C) IGF-1R immunohistochemistry.

Table I. Body weights and numbers of ACF and BCAC per colon of mice treated with AOM and/or MSG at the end of study (17 weeks of age)

Group number	Number of mice examined	Treatments		Body weight (g)	Total number of ACFs/colon	Total number of BCACs/colon
		MSG (2 mg/kg body wt)	AOM (15 mg/kg body wt)			
1 (MSG-AOM)	12	+ (4 times daily)	+ (4 times weekly)	44.82 ± 2.22[a,b,c]	78.00 ± 11.20[b]	13.83 ± 7.44[b,c]
2 (MSG-Saline)	6	+ (4 times daily)	− (saline)	52.29 ± 2.32[d]	0	0
3 (Salin-AOM)	11	− (saline)	+ (4 times daily)	36.62 ± 4.15[e]	69.27 ± 8.06[f]	5.45 ± 1.86
4 (Saline–Saline)	5	− (saline)	− (saline)	42.42 ± 0.78	0	0

[a]Mean ± SD.
[b]Significantly different from group 2 ($P < 0.001$).
[c]Significantly different from group 3 ($P < 0.001$).
[d]Significantly different from group 4 ($P < 0.001$).
[e]Significantly different from group 4 ($P < 0.01$).
[f]Significantly different from group 4 ($P < 0.001$).

Table II. Serum levels of total cholesterol, triglycerides, glucose and insulin of mice treated with AOM and/or MSG at the end of study (17 weeks of age)

Group number	Number of mice examined	Treatments		Total cholesterol (mg/dl)	Triglycerides (mg/dl)	Glucose (mg/dl)	Insulin (ng/dl)
		MSG (2 mg/kg body wt)	AOM (15 mg/kg body wt)				
1 (MSG-AOM)	12	+ (4 times daily)	+ (4 times weekly)	167.92 ± 19.96[a,b]	96.25 ± 14.38[b]	196.67 ± 34.09[b]	10.66 ± 1.31[b]
2 (MSG-Saline)	6	+ (4 times daily)	− (saline)	177.50 ± 23.09[c]	93.17 ± 12.64[c]	202.67 ± 15.24[c]	11.18 ± 1.41[c]
3 (Salin-AOM)	11	− (saline)	+ (4 times daily)	107.64 ± 18.65	49.45 ± 13.87	110.36 ± 10.48	0.49 ± 0.14
4 (Saline–Saline)	5	− (saline)	− (saline)	104.60 ± 13.69	45.20 ± 9.98	123.60 ± 11.30	0.50 ± 0.07

[a]Mean ± SD.
[b]Significantly different from group 3 ($P < 0.001$).
[c]Significantly different from group 4 ($P < 0.001$).

Discussion

As expected, the findings described suggest that development of AOM-induced precancerous lesions, BCAC, of the colon in the MSG mice with hyperinsulinemia, hypercholesterolemia, hyperglycemia and hyperlipidemia was increased, when compared with the Salin-AOM mice. Our findings are in accordance with our previous findings that AOM-induced colon carcinogenesis is enhanced in another obese model using C57BL/KsJ-db/db mice (29–31). In the current study, the number of ACF was not different between the

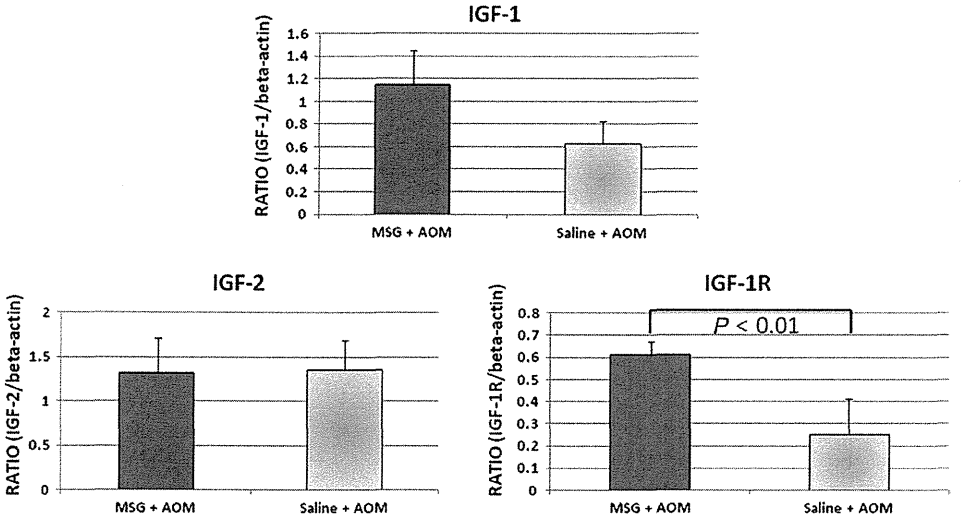

Fig. 3. mRNA expression of IGF-1, IGF-2 and IGF-1R in the colonic mucosa of the MSG-AOM mice and the Saline-AOM mice.

MSG-AOM mice and Saline-AOM mice, suggesting that BCAC rather than ACF has potential to progress to malignancies (39,42). This may be explained by the differences of pathobiological characteristics between two lesions: BCAC is dysplastic and microadenomas and ACF is consisted of hyperplastic and dysplastic lesions.

ACF have attracted attention as putative precancerous lesions in the colon in both experimental models and in humans (36). A number of molecular abnormalities, including increased expression of K-*ras* and *APC* gene mutations, are demonstrated in human ACF (46–48). BCAC, which accumulate β-catenin protein in the nucleus and cytoplasm, are also regarded as putative precursors to colorectal adenomas (37). Several rodent studies have shown that both of these lesions are useful as biomarkers to evaluate the chemopreventive properties of specific agents (49,50). In human colorectum, increased plasma IGF-1 levels are associated with the number of dysplastic ACF (51), suggesting that IGF-1 may be a promoter of the growth of dysplastic ACF and an independent risk factor of CRC. It may be possible that the number of dysplastic ACF, but not hyperplastic ACF, may be increased in the MSG-AOM mice, although we did not analyze two types of ACF.

Neonatal injections of MSG to mice or rats cause hyperthalamic damage (52,53), and as a consequence, these animals present several neuroendocrine and metabolic alterations, which lead central obesity, type 2 diabetes, insulin resistance, hyperinsulinemia, hypertriglyceridemia and hyperlipidemia (33). These abnormalities are risks for the development of CRC (9). The pancreatic islets in the mice subcutaneously injected MSG in neonatal period are hyperplastic up to 54 weeks of age (33). Therefore, our model described here may be suitable to study the pathobiology of diabetes- and obesity-associated colorectal carcinogenesis.

In this study, blood insulin level of the MSG-Saline mice (group 2) was the highest among the groups. There is accumulating evidence suggesting that hyperinsulinemia is involved in colon carcinogenesis, obesity and diabetes (3,8,9,12,54,55). Several epidemiological studies indicate that type 2 diabetic patients with hyperinsulinemia increases risk for CRC (3,12). Additionally, continuous injections of insulin promote AOM-induced colon carcinogenesis in rats (56,57). Hence, it seems likely that hyperinsulinemia in the MSG-AOM mice enhanced the development of AOM-induced lesions in the present study. Hyperglycemia and hypercholesterolemia observed in the MSG-AOM mice also contribute the development of BCAC and ACF in the colorectum because these conditions are positively associated with CRC occurrence (9,11,12). Hyperinsulinemia, hyperglycemia and hypercholesterolemia may singly or synergistically promote the development of preneoplastic and neoplastic colonic lesions. Although insulin resistance in colorectal carcinogenesis of obese people and/or type 2 diabetic patients is reported (7,55,58,59), we did not investigate presence or absence of insulin resistance in this study, Corpet *et al.* (60) reported that diet that increase some indirect insulin resistance markers does not promote colon carcinogenesis in female rats when ACF are used as a biomarker.

Regarding the mode of action, the current consensus assumes that the IGF-1 pathway plays a role in insulin-related tumor promotion in the colon (20,61). IGF-1 binds to the IGF-1R, activates a signal cascade and triggers cell proliferation in several tissues, including colon (62). Insulin at supra-physiological levels also binds to and activates the IGF-1R because of its homology with the insulin receptor (62). Furthermore, hyperinsulinemia was shown to indirectly increase bioavailability of IGF-1 by regulating levels of IGF-binding proteins (63). In this study, IGF-1R immunohistochemical expression of IGF-1 was strongly positive in the cytoplasm of BCAC developed in the MSG-AOM mice. Indeed, overexpression of IGF-1R was also reported in human CRC (64). Accordingly, it may be possible that hyperinsulinemia in MSG-AOM mice activates the signaling cascades involving the IGF-IR, resulting in a proliferative response (19,59,61). Another interesting findings regarding IGF-1R immunohistochemistry is that inflammatory cells infiltrated around BCAC were positively reacted against the IGF-1R antibody. Significance of the findings is not known, but similar findings have been reported in human Crohn's disease (65). IGF-1 and IGF2 are potentially relevant mediators in the chronic inflammation (27) and mediate the majority of their biological action through IGF-1R (66). Thus, our findings on the IGF-1R immunohistochemical positivity in inflammatory cells suggest that inflammation in the microenvironment of precancerous lesions for CRC may contribute to the growth of the lesions (67,68).

In conclusion, our data indicate that the MSG-AOM mice with hyperinsulinemia, hypercholesterolemia, hyperglycemia and hypercholesterolemia are highly susceptible to colorectal carcinogenesis and the MSG-AOM mouse model could be useful for investigating the mechanisms of obesity/diabetes-associated events involving in colorectal carcinogenesis and the therapeutic and chemopreventive strategies of CRC in obese people and/or type 2 diabetic patients.

Funding

This work was supported in part by a Grant-in-Aid from the Ministry of Health, Labour and Welfare of Japan (to Y.H.); a Grant-in-Aid for the 3rd Term Comprehensive 10-Year Strategy for Cancer Control from the Ministry of Health, Labour and Welfare of Japan (to T.T.);

a Grant-in-Aid for Cancer Research from the Ministry of Health, Labour and Welfare of Japan; and Grants-in-Aid for Scientific Research (No. 23501324) from the Ministry of Education, Culture, Sports, Science and Technology of Japan (to T.T.).

Acknowledgements

We wish to thank Kyoko Takahashi and Ayako Suga for their technical assistance and Yoshitaka Kinjo for care of the animals.

Conflict of Interest Statement: None declared.

References

1. Bergstrom,A. *et al.* (2001) Overweight as an avoidable cause of cancer in Europe. *Int. J. Cancer*, **91**, 421–430.
2. Murphy,T.K. *et al.* (2000) Body mass index and colon cancer mortality in a large prospective study. *Am. J. Epidemiol.*, **152**, 847–854.
3. Berster,J.M. *et al.* (2008) Type 2 diabetes mellitus as risk factor for colorectal cancer. *Arch. Physiol. Biochem.*, **114**, 84–98.
4. Craigie,A.M. *et al.* (2011) Study protocol for BeWEL: the impact of a BodyWEight and physicaL activity intervention on adults at risk of developing colorectal adenomas. *BMC Public Health*, **11**, 184.
5. Morita,T. *et al.* (2005) The metabolic syndrome is associated with increased risk of colorectal adenoma development: the Self-Defense Forces health study. *Asian Pac. J. Cancer Prev.*, **6**, 485–489.
6. Nilsen,T.I. *et al.* (2001) Prospective study of colorectal cancer risk and physical activity, diabetes, blood glucose and BMI: exploring the hyperinsulinaemia hypothesis. *Br. J. Cancer*, **84**, 417–422.
7. Takahashi,H. *et al.* (2007) Life style-related diseases of the digestive system: colorectal cancer as a life style-related disease: from carcinogenesis to medical treatment. *J. Pharmacol. Sci.*, **105**, 129–132.
8. Giouleme,O. *et al.* (2011) Is diabetes a causal agent for colorectal cancer? Pathophysiological and molecular mechanisms. *World J. Gastroenterol.*, **17**, 444–448.
9. Siddiqui,A.A. (2011) Metabolic syndrome and its association with colorectal cancer: a review. *Am. J. Med. Sci.*, **341**, 227–231.
10. Canani,R.B. *et al.* (2011) Potential beneficial effects of butyrate in intestinal and extraintestinal diseases. *World J. Gastroenterol.*, **17**, 1519–1528.
11. Herbey,I.I. *et al.* (2005) Colorectal cancer and hypercholesterolemia: review of current research. *Exp. Oncol.*, **27**, 166–178.
12. Chang,C.K. *et al.* (2003) Hyperinsulinaemia and hyperglycaemia: possible risk factors of colorectal cancer among diabetic patients. *Diabetologia*, **46**, 595–607.
13. Davies,M. *et al.* (2006) The insulin-like growth factor system and colorectal cancer: clinical and experimental evidence. *Int. J. Colorectal Dis.*, **21**, 201–208.
14. Durai,R. *et al.* (2005) The role of the insulin-like growth factor system in colorectal cancer: review of current knowledge. *Int. J. Colorectal Dis.*, **20**, 203–220.
15. Sandhu,M.S. *et al.* (2002) Insulin, insulin-like growth factor-I (IGF-I), IGF binding proteins, their biologic interactions, and colorectal cancer. *J. Natl Cancer Inst.*, **94**, 972–980.
16. LeRoith,D. *et al.* (2003) The insulin-like growth factor system and cancer. *Cancer Lett.*, **195**, 127–137.
17. Ewing,G.P. *et al.* (2010) The insulin-like growth factor signaling pathway as a target for treatment of colorectal carcinoma. *Clin. Colorectal Cancer*, **9**, 219–223.
18. Golan,T. *et al.* (2011) Targeting the insulin growth factor pathway in gastrointestinal cancers. *Oncology (Williston Park)*, **25**, 518–526, 529.
19. Ludwig,J.A. *et al.* (2011) Dual targeting of the insulin-like growth factor and collateral pathways in cancer: combating drug resistance. *Cancers*, **3**, 3029–3054.
20. Shimizu,M. *et al.* (2011) Cancer chemoprevention with green tea catechins by targeting receptor tyrosine kinases. *Mol. Nutr. Food Res.*, **55**, 832–843.
21. Voskuil,D.W. *et al.* (2005) The insulin-like growth factor system in cancer prevention: potential of dietary intervention strategies. *Cancer Epidemiol. Biomarkers Prev.*, **14**, 195–203.
22. Bustin,S.A. *et al.* (2001) The growth hormone-insulin-like growth factor-I axis and colorectal cancer. *Trends Mol. Med.*, **7**, 447–454.
23. Haydon,A.M. *et al.* (2006) Physical activity, insulin-like growth factor 1, insulin-like growth factor binding protein 3, and survival from colorectal cancer. *Gut*, **55**, 689–694.
24. Renehan,A.G. *et al.* (2004) Insulin-like growth factor (IGF)-I, IGF binding protein-3, and cancer risk: systematic review and meta-regression analysis. *Lancet*, **363**, 1346–1353.
25. Shimizu,M. *et al.* (2009) Supplementation with branched-chain amino acids inhibits azoxymethane-induced colonic preneoplastic lesions in male C57BL/KsJ-db/db mice. *Clin. Cancer Res.*, **15**, 3068–3075.
26. Shimizu,M. *et al.* (2008) (-)-Epigallocatechin gallate suppresses azoxymethane-induced colonic premalignant lesions in male C57BL/KsJ-db/db mice. *Cancer Prev. Res. (Phila)*, **1**, 298–304.
27. Shimizu,M. *et al.* (2011) Preventive effects of (-)-epigallocatechin gallate on diethylnitrosamine-induced liver tumorigenesis in obese and diabetic C57BL/KsJ-db/db mice. *Cancer Prev. Res. (Phila)*, **4**, 396–403.
28. Shimizu,M. *et al.* (2008) EGCG inhibits activation of the insulin-like growth factor (IGF)/IGF-1 receptor axis in human hepatocellular carcinoma cells. *Cancer Lett.*, **262**, 10–18.
29. Hirose,Y. *et al.* (2004) Enhancement of development of azoxymethane-induced colonic premalignant lesions in C57BL/KsJ-db/db mice. *Carcinogenesis*, **25**, 821–825.
30. Suzuki,R. *et al.* (2007) Diet supplemented with citrus unshiu segment membrane suppresses chemically induced colonic preneoplastic lesions and fatty liver in male db/db mice. *Int. J. Cancer*, **120**, 252–258.
31. Hayashi,K. *et al.* (2007) Citrus auraptene suppresses azoxymethane-induced colonic preneoplastic lesions in C57BL/KsJ-db/db mice. *Nutr. Cancer*, **58**, 75–84.
32. Tanaka,T. *et al.* (2008) Citrus compounds inhibit inflammation- and obesity-related colon carcinogenesis in mice. *Nutr. Cancer*, **60** (suppl. 1), 70–80.
33. Nagata,M. *et al.* (2006) Type 2 diabetes mellitus in obese mouse model induced by monosodium glutamate. *Exp. Anim.*, **55**, 109–115.
34. Sasaki,Y. *et al.* (2009) Dose dependent development of diabetes mellitus and non-alcoholic steatohepatitis in monosodium glutamate-induced obese mice. *Life Sci.*, **85**, 490–498.
35. Bird,R.P. *et al.* (2000) The significance of aberrant crypt foci in understanding the pathogenesis of colon cancer. *Toxicol. Lett.*, **112–113**, 395–402.
36. Raju,J. (2008) Azoxymethane-induced rat aberrant crypt foci: relevance in studying chemoprevention of colon cancer. *World J. Gastroenterol.*, **14**, 6632–6635.
37. Mori,H. *et al.* (2005) Significance and role of early-lesions in experimental colorectal carcinogenesis. *Chem. Biol. Interact.*, **155**, 1–9.
38. Yamada,Y. *et al.* (2001) Sequential analysis of morphological and biological properties of beta-catenin-accumulated crypts, provable premalignant lesions independent of aberrant crypt foci in rat colon carcinogenesis. *Cancer Res.*, **61**, 1874–1878.
39. Yamada,Y. *et al.* (2003) Pre-cancerous lesions for colorectal cancers in rodents: a new concept. *Carcinogenesis*, **24**, 1015–1019.
40. Yamada,Y. *et al.* (2002) Microadenomatous lesions involving loss of Apc heterozygosity in the colon of adult Apc(Min/+) mice. *Cancer Res.*, **62**, 6367–6370.
41. Hata,K. *et al.* (2006) beta-Catenin-accumulated crypts in the colonic mucosa of juvenile ApcMin/+ mice. *Cancer Lett.*, **239**, 123–128.
42. Mori,H. *et al.* (2004) Aberrant crypt foci and beta-catenin accumulated crypts; significance and roles for colorectal carcinogenesis. *Mutat. Res.*, **566**, 191–208.
43. Hirose,Y. *et al.* (2003) Azoxymethane-induced beta-catenin-accumulated crypts in colonic mucosa of rodents as an intermediate biomarker for colon carcinogenesis. *Carcinogenesis*, **24**, 107–111.
44. Mori,H. *et al.* (2002) Chemoprevention of large bowel carcinogenesis; the role of control of cell proliferation and significance of beta-catenin-accumulated crypts as a new biomarker. *Eur. J. Cancer Prev.*, **11** (suppl. 2), S71–S75.
45. Hata,K. *et al.* (2006) Lack of enhancing effects of degraded lambda-carrageenan on the development of beta-catenin-accumulated crypts in male DBA/2J mice initiated with azoxymethane. *Cancer Lett.*, **238**, 69–75.
46. Gupta,A.K. *et al.* (2007) Aberrant crypt foci: what we know and what we need to know. *Clin. Gastroenterol. Hepatol.*, **5**, 526–533.
47. Takayama,T. *et al.* (2001) Analysis of K-ras, APC, and beta-catenin in aberrant crypt foci in sporadic adenoma, cancer, and familial adenomatous polyposis. *Gastroenterology*, **121**, 599–611.
48. Kukitsu,T. *et al.* (2008) Aberrant crypt foci as precursors of the dysplasia-carcinoma sequence in patients with ulcerative colitis. *Clin. Cancer Res.*, **14**, 48–54.
49. Tanaka,T. (2009) Colorectal carcinogenesis: review of human and experimental animal studies. *J. Carcinog.*, **8**, 5.
50. Yasui,Y. *et al.* (2009) Colorectal carcinogenesis and suppression of tumor development by inhibition of enzymes and molecular targets. *Curr. Enzym. Inhib.*, **5**, 1–26.

51. Takahashi,H. *et al.* (2009) Correlation of the plasma level of insulin-like growth factor-1 with the number of aberrant crypt foci in male individuals. *Mol. Med. Report*, **2**, 339–343.
52. Holzwarth-McBride,M.A. *et al.* (1976) Monosodium glutamate induced lesions of the arcurate nucleus. II. Fluorescence histochemistry of catecholamines. *Anat. Rec.*, **186**, 197–205.
53. Nakagawa,T. *et al.* (2000) Effects of chronic administration of sibutramine on body weight, food intake and motor activity in neonatally monosodium glutamate-treated obese female rats: relationship of antiobesity effect with monoamines. *Exp. Anim.*, **49**, 239–249.
54. Mulholland,H.G. *et al.* (2009) Glycemic index, glycemic load, and risk of digestive tract neoplasms: a systematic review and meta-analysis. *Am. J. Clin. Nutr.*, **89**, 568–576.
55. Pais,R. *et al.* (2009) Metabolic syndrome and risk of subsequent colorectal cancer. *World J. Gastroenterol.*, **15**, 5141–5148.
56. Corpet,D.E. *et al.* (1997) Insulin injections promote the growth of aberrant crypt foci in the colon of rats. *Nutr. Cancer*, **27**, 316–320.
57. Tran,T.T. *et al.* (1996) Insulin promotion of colon tumors in rats. *Cancer Epidemiol. Biomarkers Prev.*, **5**, 1013–1015.
58. Bruce,W.R. *et al.* (2000) Mechanisms linking diet and colorectal cancer: the possible role of insulin resistance. *Nutr. Cancer*, **37**, 19–26.
59. Komninou,D. *et al.* (2003) Insulin resistance and its contribution to colon carcinogenesis. *Exp. Biol. Med. (Maywood)*, **228**, 396–405.
60. Corpet,D.E. *et al.* (1998) Glycemic index, nutrient density, and promotion of aberrant crypt foci in rat colon. *Nutr. Cancer*, **32**, 29–36.
61. Donohoe,C.L. *et al.* (2011) Visceral adiposity, insulin resistance and cancer risk. *Diabetol. Metab. Syndr.*, **3**, 12.
62. Adams,T.E. *et al.* (2000) Structure and function of the type 1 insulin-like growth factor receptor. *Cell. Mol. Life Sci.*, **57**, 1050–1093.
63. Attia,N. *et al.* (1998) The metabolic syndrome and insulin-like growth factor I regulation in adolescent obesity. *J. Clin. Endocrinol. Metab.*, **83**, 1467–1471.
64. Hakam,A. *et al.* (1999) Expression of insulin-like growth factor-1 receptor in human colorectal cancer. *Hum. Pathol.*, **30**, 1128–1133.
65. El Yafi,F. *et al.* (2005) Altered expression of type I insulin-like growth factor receptor in Crohn's disease. *Clin. Exp. Immunol.*, **139**, 526–533.
66. Jones,J.I. *et al.* (1995) Insulin-like growth factors and their binding proteins: biological actions. *Endocr. Rev.*, **16**, 3–34.
67. Tanaka,T. *et al.* (2006) Dextran sodium sulfate strongly promotes colorectal carcinogenesis in Apc(Min/+) mice: inflammatory stimuli by dextran sodium sulfate results in development of multiple colonic neoplasms. *Int. J. Cancer*, **118**, 25–34.
68. Tanaka,T. *et al.* (2003) A novel inflammation-related mouse colon carcinogenesis model induced by azoxymethane and dextran sodium sulfate. *Cancer Sci.*, **94**, 965–973.

Received October 7, 2011; revised December 13, 2011; accepted December 27, 2011

J Gastroenterol (2012) 47:321–333
DOI 10.1007/s00535-011-0484-9

ORIGINAL ARTICLE—LIVER, PANCREAS, AND BILIARY TRACT

Glycogen synthase kinase 3β inhibition sensitizes pancreatic cancer cells to gemcitabine

Takeo Shimasaki · Yasuhito Ishigaki · Yuka Nakamura · Takanobu Takata · Naoki Nakaya · Hideo Nakajima · Itaru Sato · Xia Zhao · Ayako Kitano · Kazuyuki Kawakami · Takuji Tanaka · Tsutomu Takegami · Naohisa Tomosugi · Toshinari Minamoto · Yoshiharu Motoo

Received: 1 March 2011 / Accepted: 16 September 2011 / Published online: 1 November 2011

Abstract

Background Pancreatic cancer is obstinate and resistant to gemcitabine, a standard chemotherapeutic agent for the disease. We previously showed a therapeutic effect of glycogen synthase kinase-3β (GSK3β) inhibition against gastrointestinal cancer and glioblastoma. Here, we investigated the effect of GSK3β inhibition on pancreatic cancer cell sensitivity to gemcitabine and the underlying molecular mechanism.

Methods Expression, phosphorylation, and activity of GSK3β in pancreatic cancer cells (PANC-1) were examined by Western immunoblotting and in vitro kinase assay. The combined effect of gemcitabine and a GSK3β inhibitor (AR-A014418) against PANC-1 cells was examined by isobologram and PANC-1 xenografts in mice. Changes in gene expression in PANC-1 cells following GSK3β inhibition were studied by cDNA microarray and reverse transcription (RT)-PCR.

Results PANC-1 cells showed increased GSK3β expression, phosphorylation at tyrosine 216 (active form), and activity compared with non-neoplastic HEK293 cells. Administration of AR-A014418 at pharmacological doses attenuated proliferation of PANC-1 cells and xenografts, and significantly sensitized them to gemcitabine. Isobologram analysis determined that the combined effect was synergistic. DNA microarray analysis detected GSK3β inhibition-associated changes in gene expression in gemcitabine-treated PANC-1 cells. Among these changes, RT-PCR and Western blotting showed that expression of tumor protein 53-induced nuclear protein 1, a gene regulating cell death and DNA repair, was increased by gemcitabine treatment and substantially decreased by GSK3β inhibition.

Conclusions The results indicate that GSK3β inhibition sensitizes pancreatic cancer cells to gemcitabine with altered expression of genes involved in DNA repair. This study provides insight into the molecular mechanism of gemcitabine resistance and thus a new strategy for pancreatic cancer chemotherapy.

Keywords Pancreatic cancer · Gemcitabine · Glycogen synthase kinase 3β · TP53INP1

Abbreviations

ABC	Avidin–biotin peroxidase complex
ATP	Adenosine triphosphate

Electronic supplementary material The online version of this article (doi:10.1007/s00535-011-0484-9) contains supplementary material, which is available to authorized users.

T. Shimasaki (✉) · N. Nakaya · H. Nakajima · I. Sato · Y. Motoo
Department of Medical Oncology, Kanazawa Medical University, 1-1 Daigaku, Uchinada, Ishikawa 920-0293, Japan
e-mail: takeo@kanazawa-med.ac.jp

T. Shimasaki · A. Kitano · K. Kawakami · T. Minamoto
Division of Translational and Clinical Oncology, Cancer Research Institute, Kanazawa University, 13-1 Takara-machi, Kanazawa, Ishikawa 920-0934, Japan

Y. Ishigaki · Y. Nakamura · T. Takata · T. Takegami · N. Tomosugi
Medical Research Institute, Kanazawa Medical University, 1-1 Daigaku, Uchinada, Ishikawa 920-0293, Japan

X. Zhao
Institute of Pathology, Tongji Hospital, Tongji Medical College, Huazhong University of Science and Technology, Wuhan, People's Republic of China

T. Tanaka
Department of Pathology, Kanazawa Medical University, 1-1 Daigaku, Uchinada, Ishikawa 920-0293, Japan

BSA	Bovine serum albumin
cDNA	Complementary DNA
cRNA	Complementary RNA
DMSO	Dimethyl sulfoxide
EGFR	Epidermal growth factor receptor
FBS	Fetal bovine serum
GSK3β	Glycogen synthase kinase 3β
IC_{50}	50% inhibitory concentration
MAPK	Mitogen-activated protein kinase
mTOR	Mammalian target of rapamycin
NF-κB	Nuclear factor-κB
NRIKA	Non-radioisotopic in vitro kinase assay
p53DINP1	p53-dependent damage-inducible nuclear protein 1
PBS	Phosphate buffered saline
PCNA	Proliferating cell nuclear antigen
PDGF	Platelet-derived growth factor receptor
PI3K	Phosphatidylinositol 3-kinase
RNAi	RNA interference
RR	Ribonucleotide reductase
RT-PCR	Reverse transcription-polymerase chain reaction
SD(s)	Standard deviation(s)
SIP	Stress-induced protein
siRNA	Small interfering RNA
TEAP	Thymus-expressed acidic protein
TK	Thymidine kinase
TP53INP1	Tumor protein 53-induced nuclear protein 1
TS	Thymidylate synthase
TUNEL	Terminal deoxynucleotidyl transferase-mediated dUTP nick end labeling
VEGF	Vascular endothelial growth factor
VEGFR	VEGF receptor
WST-8	4-[3-(4-Iodophenyl)-2-(4-nitrophenyl)-2*H*-5-tetrazolio]-1,3-benzene disulfonate

Introduction

Pancreatic cancer is the fourth and fifth leading cause of cancer death in the USA and Japan, respectively [1–4]. Early diagnosis is difficult and metastasis is frequently found during primary tumor diagnosis. Biologically, this tumor is characterized by highly proliferative and invasive activity, and its aggressive nature is an obstacle to early diagnosis and curative surgical intervention [5, 6]. Gemcitabine is a deoxycytidine analog widely used as a standard anticancer drug in the treatment of pancreatic cancer, but it is effective in less than 20% of patients [3, 4, 7]. Radiation therapy alone or in combination with gemcitabine is insufficient for improving survival of pancreatic cancer patients [5, 6]. For this reason, there is an urgent need for new treatment modalities for pancreatic cancer, such as molecular-target directed therapies.

Accumulating molecular studies have elucidated a complex genetic mechanism of cancer that involves multidirectional signal transduction pathways [8]. The major axis of signal transduction includes the RAS/mitogen-activated protein kinase (MAPK), phosphatidylinositol 3-kinase (PI3K)/Akt/mammalian target of rapamycin (mTOR), and hedgehog pathways, and plays an important role in the development and progression of pancreatic cancer [9]. Tyrosine kinases such as the epidermal growth factor receptor (EGFR), vascular endothelial growth factor receptor (VEGFR), and platelet-derived growth factor receptor (PDGFR) are targeted in cancer treatment because they are overexpressed in many tumors, including pancreatic cancer [10]. Currently available agents targeting these molecules are anti-EGFR antibodies (cetuximab, panitumumab), small-molecule EGFR inhibitors (gefitinib, erlotinib), an anti-VEGF antibody (bevacizumab), and a small-molecule VEGFR inhibitor (axitinib). A number of phase III clinical trials have been conducted using either kinase inhibitors alone or in combination with gemcitabine for treating pancreatic cancer patients. Other than a combination of erlotinib and gemcitabine [11], these trials have shown little therapeutic benefit to the patients enrolled (reviewed in Ref. [12]). Therefore, identification of new molecular target(s) is necessary for developing a therapeutic strategy that enhances the effect of gemcitabine and thus improves patient survival.

Among serine/threonine protein kinases, glycogen synthase kinase 3β (GSK3β) has emerged as a clue to understanding the molecular mechanism of chronic, progressive diseases, and thus as a potential therapeutic target [13]. On the basis of its known biological properties and functions [14–16] as well as its involvement in primary pathologies [13], GSK3β has been a target of drug development for non-insulin-dependent diabetes mellitus, Alzheimer's disease, osteoporosis, and inflammation [13, 17, 18]. We recently demonstrated that deregulated GSK3β expression and activity are characteristic of gastrointestinal cancer (including pancreatic cancer) and glioblastoma, and that GSK3β maintains survival and proliferation of these tumor cells. The pathologic role of GSK3β in cancer is supported by our findings that inhibition of this kinase attenuates survival and proliferation, and induces apoptosis of the tumor cells and their xenografts [19–22]. The antitumor effect of GSK3β inhibition is associated with (re)activation of p53- and Rb-mediated pathways and attenuated cell immortality activity [21, 22].

Concurrent with and following our studies on the antitumor effects of GSK3β inhibition, similar observations were reported in various cancer types (reviewed in

Ref. [23]). Based on studies indicating possible involvement of GSK3β in the nuclear factor-κB (NF-κB)-mediated cell survival pathway [24, 25], a number of studies have shown that GSK3β participates in pancreatic cancer cell survival via the NF-κB pathway [26–28]. Few studies had focused on whether GSK3β inhibition sensitizes cancer cells to chemotherapeutic agents until we found that GSK3β inhibition sensitizes glioblastoma cells to chemotherapeutic agents (e.g., temozolomide, ACNU) and ionizing radiation [23]. In this study, we investigated the effect of GSK3β inhibition on pancreatic cancer cell sensitivity to gemcitabine and the underlying molecular mechanism.

Materials and methods

Cell lines

Human pancreatic cancer cells (PANC-1) and human embryonic kidney cells (HEK293) were obtained from American Type Culture Collection (Manassas, VA, USA). Since HEK293 cells stop growing due to contact inhibition, we considered these to be the non-neoplastic cell line in our experiments. Cells were cultured in Dulbecco's Modified Eagle's Medium containing 10% fetal bovine serum (FBS; GIBCO, Carlsbad, CA, USA) at 37°C under 5% CO_2 and harvested for extraction of cellular protein and nucleic acids.

Expression and phosphorylation of cellular GSK3β

We extracted cellular protein from a frozen pellet of cells using lysis buffer (CelLytic^{TM}-MT, Sigma-Aldrich, St. Louis, MO, USA) containing a mixture of protease and phosphatase inhibitors (both from Sigma-Aldrich). A 50-μg aliquot of protein extract was subjected to Western immunoblotting analysis as described previously [19, 29] to examine expression and phosphorylation of GSK3β using primary antibodies (at the dilution shown) against total GSK3 (GSK3α and β; 1:1,000; Upstate Biotechnology, Lake Placid, NY, USA), GSK3β (1:2,500; BD Biosciences, Lexington, KY, USA), GSK3β phosphorylated at serine 9 (pGSK3β^{S9}:1,000; Cell Signaling Technology, Beverly, MA, USA) and at tyrosine 216 (pGSK3β^{Y216}; 1:1,000; BD Biosciences). In each case, the signal was developed using an enhanced chemiluminescent detection reagent (ECL®, Amersham, Little Chalfont, UK). The amount of protein in each sample was monitored by expression of β-actin (1:1,000; Ambion, Woodward-Austin, TX, USA).

Non-radioisotopic in vitro kinase assay

We detected cellular GSK3β activity using the non-radioisotopic in vitro kinase assay (NRIKA) according to the method in our previous report [30]. GSK3β was isolated from 1-mg aliquots of each sample cell lysate by immunoprecipitation, and then used in the in vitro kinase reaction in the presence of its substrate, recombinant human β-catenin protein (β-catenin^{His}), and non-radioisotopic adenosine triphosphate (ATP). We analyzed the products by Western immunoblotting for phosphorylated β-catenin^{His} using an antibody to β-catenin phosphorylated at serine 33 and 37 and/or threonine 41 (p-β-catenin$^{S33/37/T41}$; Cell Signaling Technology). As a negative control (NC) for each cell line, the mouse monoclonal antibody to GSK3β was replaced by an equal amount of non-immune mouse IgG in the immunoprecipitation step. Cellular GSK3β activity is demonstrated by p-β-catenin$^{S33/37/T41}$ expression in the test lanes (T), and little or no expression of p-β-catenin$^{S33/37/T41}$ in the NC. The amount of GSK3β and the presence of β-catenin^{His} in the kinase reaction were monitored by immunoblotting with mouse monoclonal antibodies to GSK3β and β-catenin (1:1,000; BD Biosciences), respectively.

Effects of gemcitabine and GSK3β inhibition on cancer cell survival

Cells seeded in 96-well culture plates at a density of 1×10^4 cells/mL were treated with dimethyl sulfoxide (DMSO), gemcitabine (generously provided by Eli Lilly Co., Ltd., Tokyo, Japan), or a small-molecule GSK3β inhibitor (AR-A014418; Calbiochem®, EMD Bioscience, San Diego, CA, USA) dissolved in DMSO at the indicated final concentrations in the medium. Concentrations of AR-A014418 used in this study (10 and 25 μM) are within the pharmacologically relevant range previously reported [31]. We tested each concentration or combination of agents in four wells, and performed the experiments three times. At designated time points, relative numbers of viable cells were determined using a WST-8 (4-[3-(4-iodophenyl)-2-(4-nitrophenyl)-2*H*-5-tetrazolio]-1,3-benzene disulfonate) assay kit (Wako, Japan) and a spectrophotometer (ELx800; BioTek Instruments, Winooski, VT, USA). We used these numbers to calculate 50% inhibitory concentrations (IC_{50}) of gemcitabine and AR-A014418, and to generate an isobologram that allows evaluation of whether the effect of the two drugs in combination is additive, synergistic, or antagonistic [32].

RNA interference for GSK3β and tumor protein 53-induced nuclear protein 1 (TP53INP1)

The effect of depletion of GSK3β or TP53INP1 on PANC-1 cell viability and sensitivity to gemcitabine was examined by RNA interference (RNAi) using the small interfering RNA (siRNA) specific to GSK3β (Validated Stealth RNAi,

OligoID VHS40271, Invitrogen, Carlsbad, CA, USA) or TP53INP1 (Oligo ID HSS150786, Invitrogen). Specific effects of RNAi on expression of mRNA and protein of these molecules were confirmed respectively by quantitative reverse transcription (RT)-PCR (data not shown) and Western immunoblotting by using antibodies to total GSK3 (GSK3α and β; 1:1,000; Upstate Biotechnology) and TP53INP1 (1:1,000; abcam, Cambridge, MA, USA). PANC-1 cells were treated by transfection with either GSK3β-specific (10 nM) or TP53INP1-specific siRNA (10 nM) alone, or in combination with gemcitabine (50 mg/mL, 190 μM). As controls, the cells were treated with PBS and the nonspecific siRNA (Stealth RNAi^{TM} siRNA Negative Control Med GC [12935-300], Invitrogen). At 48 h after the respective treatment, relative numbers of viable cells were measured by a WST-8 assay. Each assay was done in four wells three times.

Experimental animal study

Pathogen-free 6-week-old female athymic nude mice (BALB/c) were supplied by JAPAN SLC (Hamamatsu, Japan). After quarantine for 2–3 weeks in pathogen-free conditions at the Animal Experiment Facility in the Advanced Science Research Center of the Kanazawa Medical University, these mice were inoculated with PANC-1 cells and subsequently treated according to the design and protocol shown in Fig. 1a. Four weeks after inoculation, 32 mice with PANC-1 xenografts were assigned to four treatment groups. These groups were given intraperitoneal injections of 200 μL 75% DMSO, gemcitabine (20 mg/kg body weight), AR-A014418 (2 mg/kg body weight), or a mixture of both agents dissolved in 200 μL DMSO, respectively, two times a week for 8 weeks. Doses of AR-A014418 and gemcitabine corresponded to concentrations of 10 and 120 μM, respectively, in culture media used in the in vitro treatment of cells [20, 22]. Our pilot study using SW480 and HT29 colon cancer cell xenografts [20, 22] estimated the AR-A014418 dose corresponding to a concentration used previously in the in vitro treatment of cells [19, 21, 22]. Assuming that total body fluid accounts for approximately 60% of a mouse's body weight, an inhibitor dose of 2 mg/kg body weight corresponds to a concentration of approximately 10 μM in culture media [20], which is known to be a pharmacological dose for AR-A014418 [31]. Throughout the experiment, we carefully observed all mice daily for adverse events and measured tumors every week. Tumor volume (cm^3) was calculated using the formula $0.5 \times S^2 \times L$, where S is the smallest tumor diameter (cm) and L is the largest (cm) [20]. Body weights of animals were monitored during the treatment (Fig. 1b). All mice were euthanized at 12 weeks after completion of treatment. At necropsy, tumor xenografts and the major vital organs (lungs, liver, gastrointestinal tract, pancreas, kidneys, and spleen) were removed, fixed in 10% neutral buffered formalin and embedded in paraffin for histopathologic, histochemical, and immunohistochemical examination. Paraffin sections of these tumors were stained with hematoxylin and eosin (HE) for histopathologic examination. All experiments were conducted according to the Guidelines for the Care and Use of Laboratory Animals in Kanazawa Medical University, and in accordance with national guidelines for animal use in research in Japan (http://www.lifescience.mext.go.jp/policies/pdf/an_material011.pdf).

Immunohistochemical and histochemical examinations

We examined the expression of proliferating cell nuclear antigen (PCNA) in tumor xenografts from the mice by using a rabbit polyclonal antibody to PCNA (1:100; clone ID SC-7907, Santa Cruz Biotechnology, Santa Cruz, CA, USA) detected by the avidin–biotin–peroxidase complex (ABC) method, with modifications [20, 29]. For the negative control, the primary antibody was replaced by nonimmune rabbit IgG (DakoCytomation, Glostrup, Denmark). Apoptosis was detected in tumor xenografts by terminal deoxynucleotidyl transferase-mediated dUTP nick end labeling (TUNEL) using an in situ apoptosis detection TUNEL kit (Takara, Kusatsu, Japan). Frequency of proliferating cells and of apoptosis in the tumors was calculated as described previously [20]. Six optical fields, approximately 500–700 cells, were counted in each group by light microscopy under high-power magnification (400×). The number of positive cells was calculated per 500 cells.

cDNA microarray analysis

We treated PANC-1 cancer cells with gemcitabine (190 μM) and AR-A014418 (10 μM) alone or in combination, or with PBS as a control for 24, 48, and 72 h. Total RNA was isolated from these cells using the RNeasy Mini Kit (QIAGEN GmbH, Hilden, Germany). Labeled cRNA was synthesized from sample RNA using a MessageAmp® II-Biotin Enhanced Kit (Ambion) according to the manufacturer's instructions. Target hybridizations were performed on a Human Genome U133 plus 2.0 GeneChip microarray system (Affymetrix, High Wycombe, UK) in a GeneChip® Hybridization Oven 640 for 16 h at 45°C. The hybridized cRNAs were washed and stained in a GeneChip® Fluidics Station 450, and the resulting signal was detected using a GeneChip® Scanner 3000. Digitalized image data were processed using the GeneChip® Operating Software (GCOS) version 1.4. Amounts of probe-specific transcripts were determined on the basis of the average of

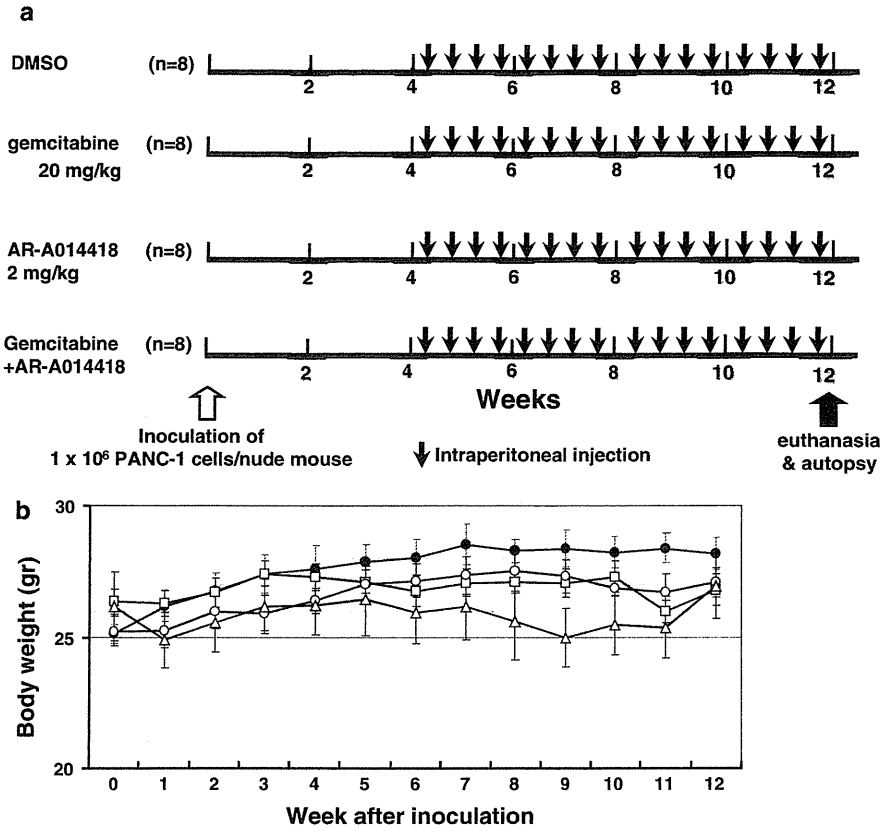

Fig. 1 Design and protocol of animal experiments, and changes in body weight of animals during treatment. **a** Pathogen-free 6-week-old female athymic mice (BALB/c, nu/nu) were quarantined for 3 weeks in pathogen-free conditions. At week 0, 1×10^6 PANC-1 human pancreatic cancer cells suspended in 50 μL of phosphate buffered saline (PBS) were inoculated subcutaneously into each of 32 mice. Four weeks after inoculation, visible subcutaneous tumors formed in all mice and were size-matched. Mice were randomly assigned to four treatment groups: DMSO (a solvent for the GSK3β inhibitor), gemcitabine, the small-molecule GSK3β inhibitor AR-A014418, and a combination of gemcitabine and the inhibitor, as described in "Materials and methods". **b** Effects of intraperitoneal injection of the agents on body weights of mice during the course of treatment. Results are shown for the groups of mice treated with the agents described in **a**. DMSO, *closed circle*; gemcitabine, *open square*; AR-A014418, *open circle*; gemcitabine and AR-A014418 in combination, *open triangle*

the differences between the perfect-match and mismatch intensities. Signal intensities of selected genes that were upregulated or downregulated fourfold compared with the control group were extracted by the GeneSpring GX software package version 7.3.1 (Agilent Technologies, Santa Clara, CA, USA).

RNA purification and quantitative real-time RT-PCR

Total RNA was extracted using the miRNeasy Kit (Qiagen) following the manufacturer's instructions. Reverse transcription of RNA to cDNA was carried out using the Taqman Reverse Transcription Reagents Kit (Applied Biosystems). Expression levels of TP53INP1 and β-actin (ACTB) were quantified using Taqman FAM/MGB probes on an ABI 7900HT Fast Real-Time PCR System (Applied Biosystems). TP53INP1 PCR products were detected using the Taqman Gene Expression assays (assay ID: Hs01374570_m1, Applied Biosystems). Human ACTB (P/N: 4333762T, Applied Biosystems) was used as an endogenous control. Relative quantitation was carried out using the ΔΔCt method with human ACTB as an endogenous control.

Statistical analysis

The Student's t test was used to determine statistical differences in cell survival between cells treated with DMSO, AR-A014418, and gemcitabine. In the microarray analysis, we used Fisher's exact test to calculate p values to determine the probabilities that the biological functions assigned to the different networks could be explained by chance alone. Body weights of mice and tumor volumes in each treatment group were expressed as mean ± standard deviation (SD). The statistical significance of differences

among the data was determined with one-way ANOVA followed by Fisher's PLSD post hoc test.

Results

Expression, phosphorylation, and activity of GSK3β in cancer cells

Western immunoblotting showed that PANC-1 cells had higher basal levels of GSK3β and pGSK3β^{Y216} (active form), and a lower level of pGSK3β^{S9} (inactive form) than HEK293 cells (Fig. 2a). PANC-1 cells also showed a higher level of GSK3β expression than HEK293 cells in the immunoprecipitated material, and the NRIKA showed that PANC-1 cell-derived GSK3β was active for phosphorylating β-catenin (Fig. 2b). These results are consistent with our previous findings in gastrointestinal cancer cells and tissues [19, 22]. The above characteristics of GSK3β suggested it plays a pathologic role in pancreatic cancer cells. Therefore, we investigated possible effects of inhibiting GSK3β activity on pancreatic cancer cell viability and gemcitabine sensitivity.

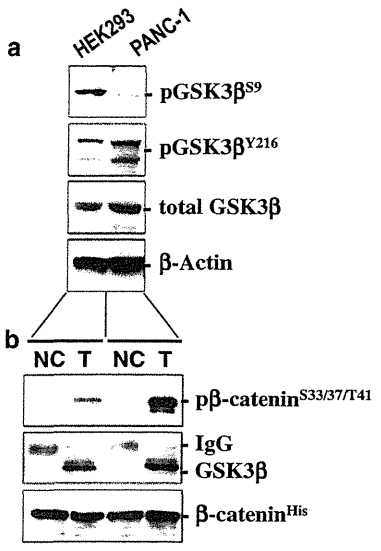

Fig. 2 Expression, phosphorylation, and activity of GSK3β in the two cell lines. **a** Protein extracts from HEK293 and PANC-1 cells were analyzed by Western immunoblotting for GSK3β expression and levels of pGSK3β^{S9}, pGSK3β^{Y216}, and β-actin. **b** GSK3β activity was detected by NRIKA [30] in HEK293 and PANC-1 cells. An in vitro kinase reaction was carried out in the presence of immunoprecipitated GSK3β from cell lysate, β-catenin^{His}, and non-radioisotopic ATP. The resultant products were analyzed by Western immunoblotting for phosphorylation of β-catenin^{His} (p-β-catenin$^{S33/37/T41}$). As a negative control (*NC*) for each cell line, the antibody to GSK3β was replaced by non-immune mouse IgG in the immunoprecipitation. GSK3β activity was shown in the cells by presence of p-β-catenin$^{S33/37/T41}$ in the test lanes (*T*) and by little or no pβ-catenin$^{S33/37/T41}$ in NC lanes. The amount of immunoprecipitated GSK3β and the presence of β-catenin^{His} were evaluated by immunoblotting with the respective specific antibodies

Effect of gemcitabine and a GSK3β inhibitor on cancer cell survival

Treatment with increasing concentrations of either gemcitabine (38, 190, and 380 μM corresponding to 10, 50, and 100 mg/mL, respectively) or AR-A014418 (10 and 25 μM) suppressed viability of PANC-1 cells in a dose- and time-dependent manner (Fig. 3). The IC_{50} of gemcitabine and AR-A014418 was 225 and 12 μM, respectively, at 48 h after treatment. We then addressed whether GSK3β inhibition could enhance the effect of gemcitabine, presently recognized as the standard treatment for pancreatic cancer.

As shown in Fig. 3, AR-A014418 alone at a dose of 25 μM had a therapeutic effect against PANC-1 cell survival that was equivalent to or higher than that of gemcitabine alone at a dose of 380 μM (100 mg/mL). Then, we tested for possible effects of 10 μM AR-A014418, a dose similar to its IC_{50}, in combination with gemcitabine at different concentrations. We observed significantly reduced cell viability at 72 and/or 48 h when PANC-1 cells were treated with a combination of 10 μM AR-A014418 and gemcitabine at a dose of 38 μM (10 mg/L), 190 μM (50 mg/L), or 380 μM (100 mg/L) compared with treatment with gemcitabine or 10 μM AR-A014418 alone (Fig. 4a–c). Isobologram analysis [32] was used to evaluate whether 10 μM AR-A014418 enhances the effect of gemcitabine against PANC-1 cells at 48 h after treatment. Analysis determined that the combined effect of 10 μM AR-A014418 and 190 μM (50 mg/L) gemcitabine was synergistic (Fig. 4d). In addition, the combination of gemcitabine (50 mg/L, 190 μM) with GSK3β RNAi yielded a lower rate of PANC-1 cell survival than either treatment alone (Fig. 5).

Effects of gemcitabine and GSK3β inhibitor on PANC-1 xenografts

The four groups of mice with PANC-1 xenografts were treated with intraperitoneal injections of DMSO, gemcitabine (20 mg/kg), AR-A014418 (2 mg/kg), and a mixture of the latter two agents, respectively, twice a week for 8 weeks (Figs. 1a, 6a). All mice tolerated the respective agents well for the 8-week treatment. Beginning 4 weeks into treatment (from week 8 in Fig. 6a), mice treated with AR-A014418 alone and in combination with gemcitabine showed significantly decreased tumor proliferation. During weeks 4–8 of treatment (weeks 8–12 in Fig. 6a), Fischer's PLSD post hoc test showed significant differences in tumor volume between the four groups of mice. Compared with mice treated with DMSO, significant antitumor effects

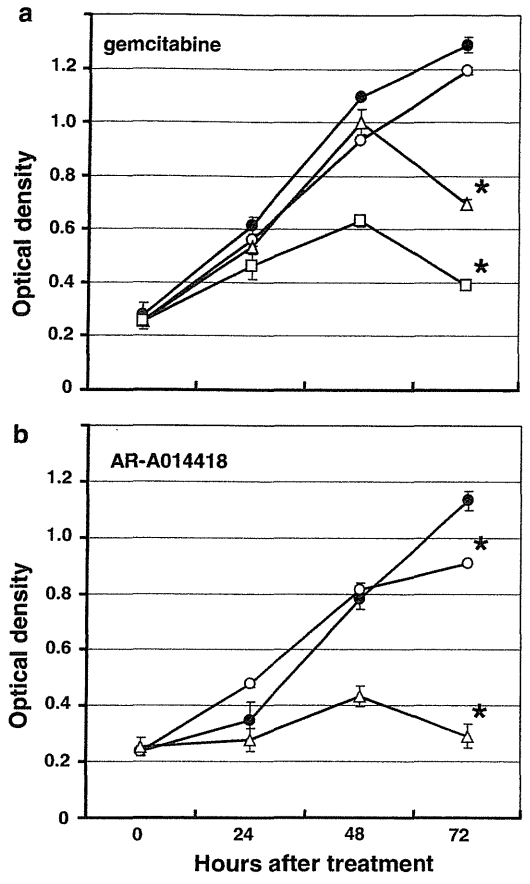

Fig. 3 Effects of gemcitabine and AR-A014418 on PANC-1 cell survival. **a** PANC-1 cells treated with PBS (*closed circle*) and gemcitabine at 10 mg/mL (38 μM; *open circle*), 50 mg/mL (190 μM; *open triangle*), and 100 mg/mL (380 μM; *open square*). **b** PANC-1 cells treated with DMSO (*closed circle*) and AR-A014418 at 10 μM (*open circle*) and 25 μM (*open triangle*). **a**, **b** The relative number of viable cells at each time point was measured by WST-8 assay. Each assay was done in six wells and performed three times. All values shown are means with SDs. *Asterisks* indicate statistically significant differences ($p < 0.01$) between cells treated with PBS and gemcitabine, and between cells treated with DMSO and AR-A014418

were found in mice treated with the following agents in order of decreasing effect: a combination of the two agents, AR-A014418 alone, and gemcitabine alone.

We observed no serious adverse events in the four groups of mice during treatment, and there were no statistically significant differences in mean body weight between the groups (Fig. 1b). At necropsy, gross observation and histological examination showed no lesions, primary tumors, or metastatic PANC-1 tumors in the major vital organs of any of the mice.

Histological examination of the tumors showed medullary proliferation of cancer cells in all cases (Fig. 6b). Histochemical (TUNEL) and immunohistochemical (PCNA) examinations of the tumor xenografts showed an increase in TUNEL-positive (apoptotic) cells and a decrease in PCNA-positive (proliferating) cells in tumors treated with gemcitabine, AR-A014418, and their combination (Fig. 6b, c).

Changes in gene expression in PANC-1 cells treated with gemcitabine and a GSK3β inhibitor

To find a molecular mechanism by which GSK3β inhibition enhances the antitumor effect of gemcitabine, we generated and compared gene expression profiles of PANC-1 cells sham (PBS)-treated and those treated with gemcitabine alone (Electronic Supplementary Material: a [24 h], b [48 h], c [72 h]) and in combination with AR-A014418 for 72 h (Electronic Supplementary Material: d [72 h]). Transcriptome comparison by cDNA microarray analysis showed significant changes in expression of numerous genes in gemcitabine-treated PANC-1 cells compared with sham-treated cells. Interestingly, the degree of change in the transcriptome profile of cells treated with a combination of gemcitabine and AR-A014418 was less marked than that of cells treated with gemcitabine alone for 72 h (Fig. 7a). This suggests that treatment with AR-A014418 counteracts gemcitabine-induced changes in gene expression in PANC-1 cells, and allows us to hypothesize that the gemcitabine-induced genes are associated with the cancer cells' resistance to this drug.

We detected three groups of genes. Group A included 84 genes that were upregulated more than fourfold at 24, 48, or 72 h after treatment with gemcitabine and downregulated less than onefold at 72 h after treatment with gemcitabine in combination with AR-A014418. Group B included 267 genes downregulated less than onefold with gemcitabine treatment and upregulated more than fourfold in combination with AR-A014418 at the same time points. Group C included 112 genes upregulated one- to fourfold with gemcitabine treatment and more than eightfold in combination with AR-A014418 at the same time points (Table 1, Supplementary Table 1). The 10 genes in each group with the most marked change in expression are shown in Table 1. With respect to gene ontology, many of these genes function in cell cycle regulation, growth, death, and cell signaling. Group A genes are likely associated with or responsible for increased sensitivity of PANC-1 cells to gemcitabine in combination with AR-A014418.

Among the representative genes in group A, we focused on tumor protein p53-induced nuclear protein 1 (TP53INP1), since our previous study demonstrated an increase in TP53INP1 protein in pancreatic cancer cells that have acquired resistance to gemcitabine [33]. Quantitative RT-PCR analysis showed that, in comparison with sham-treated PANC-1 cells, TP53INP1 mRNA expression

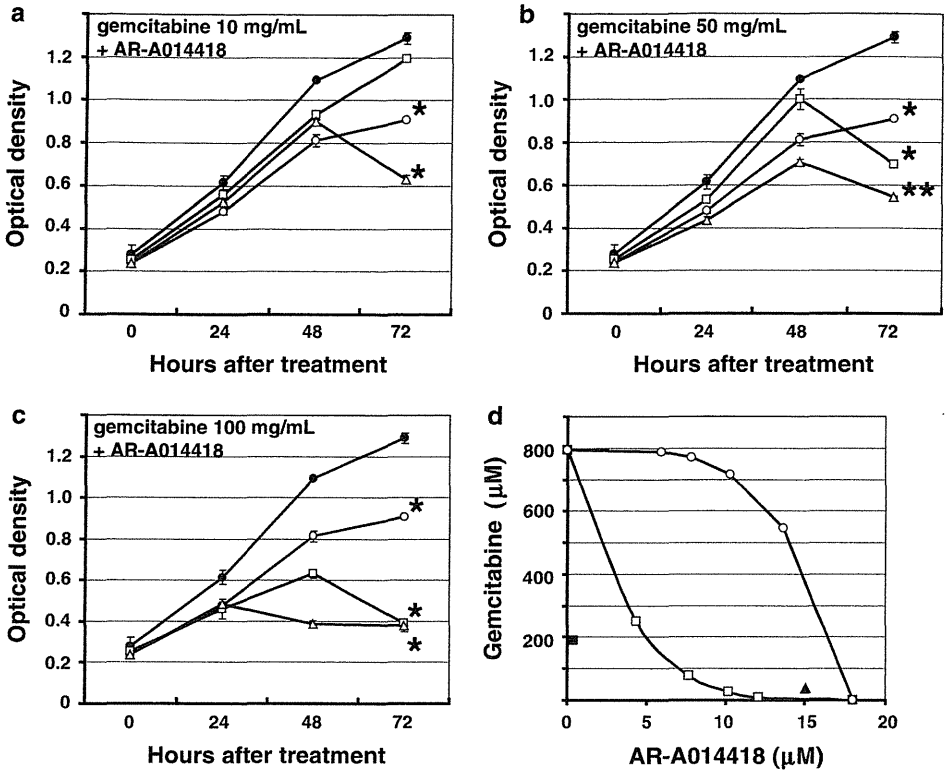

Fig. 4 Combined effect of gemcitabine and low-dose AR-A014418 on pancreatic cancer cells (PANC-1). **a–c** The relative number of viable cells at each time point was measured by WST-8 assay for PANC-1 cells treated with DMSO (*closed circle*), 10 μM AR-A014418 (*open circle*), gemcitabine at the indicated concentrations alone (*open square*) and in combination with 10 μM AR-A014418 (*open triangle*). Each assay was done in six wells and performed three times. All values shown are mean with SDs. *Asterisks* indicate statistically significant differences ($*p < 0.01$, $**p < 0.001$) between cells treated with DMSO and either gemcitabine, AR-A014418 or the two agents in combination. **d** The influence of 10 μM AR-A014418 on the effect of gemcitabine against pancreatic cancer cells was analyzed using an isobologram [32] where the IC_{50} of the combination therapy was plotted (*filled triangle*). The analysis showed that 10 μM AR-A014418 (*closed square*) synergistically enhanced the effect of gemcitabine against PANC-1 cells

increased in cells treated with gemcitabine alone and decreased in cells treated with gemcitabine in combination with AR-A014418 (Fig. 7b). This result suggests a putative role for TP53INP1 in the GSK3β inhibition-mediated enhancement of gemcitabine's effect against pancreatic cancer cells. Consistent with this observation, depletion of TP53INP1 by RNAi (Fig. 7c) significantly enhanced the effect of gemcitabine (50 mg/mL, 190 μM) in PANC-1 cell survival (Fig. 7d).

Discussion

While gemcitabine remains a standard chemotherapeutic agent for treating pancreatic cancer, the development of strategies for enhancing its antitumor effect is an urgent and important issue for improving response rate. Several trials using agents targeting oncogenic signaling pathways mediated by receptor-type tyrosine kinases have failed to improve the experimental or clinical effect of gemcitabine [10, 12]. Recent studies have found that GSK3β inhibition exerts therapeutic effects against various cancers, including pancreatic cancer, with little adverse effect (reviewed in Ref. [23]). Among them, only our study showed that inhibition of GSK3β sensitizes human glioblastoma cells to temozolomide and ionizing radiation in vitro [21]. In the present study, we demonstrated both in vitro (cell culture) and in vivo (tumor xenografts) that inhibition of deregulated GSK3β activity by its pharmacological inhibitor AR-A014418 not only attenuates survival and proliferation of pancreatic cancer cells, but also sensitizes them to gemcitabine. Consistent with our previous studies on the effects of GSK3β inhibition on non-neoplastic cells and rodents [19–22], we observed no detrimental effects of treating PANC-1 xenograft-bearing athymic mice with a pharmacological dose of AR-A014418 for 8 weeks. These results indicate that GSK3β inhibition combined with chemotherapy is a novel and promising strategy for sensitizing pancreatic cancer cells to gemcitabine.

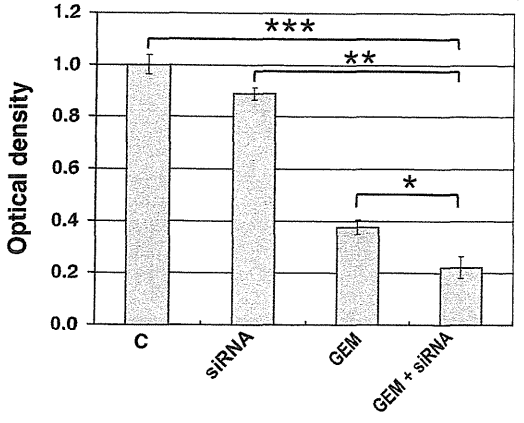

Fig. 5 Effect of gemcitabine, GSK3β-specific siRNA, and the two agents in combination in PANC-1 cells. Cells were treated with gemcitabine (50 mg/mL, 190 μM), GSK3β-specific siRNA (final concentration, 10 nM), and the two agents in combination. As a control, cells were treated with PBS and non-specific siRNA (10 nM). The relative number of viable cells at 48 h after each treatment was measured by the WST-8 assay. Each assay was done in four wells three times. Data are presented as mean ± SD. *Asterisks* indicate statistically significant differences ($*p < 0.05$; $**p < 0.01$; $***p < 0.001$) between cells treated with control (*C*; PBS and non-specific siRNA), gemcitabine (*GEM*), and GSK3β-specific siRNA (*siRNA*), and the two agents in combination (*GEM + siRNA*)

There have been many studies investigating molecular and biological mechanisms by which pancreatic cancer cells resist or acquire resistance to chemotherapy and radiation [34–36]. These studies found no decisively efficient means for overcoming pancreatic cancer cell resistance to gemcitabine and radiation. It was previously reported that GSK3β sustains pancreatic cancer cell survival by maintaining transcriptional activity of NF-κB [26, 27]. However, a recent study failed to demonstrate that disruption of NF-κB activity by inhibiting GSK3β sensitizes PANC-1 cells to gemcitabine [28]. We previously found no effect of GSK3β inhibition on endogenous NF-κB transcriptional activity in gastrointestinal cancers (including pancreatic cancer) and glioblastoma [21, 22]. Therefore, a role for GSK3β in regulating NF-κB activity is controversial.

We observed in a preliminary study that short-term gemcitabine treatment induces mesenchymal cell-like phenotypic change in pancreatic cancer cells. This change in phenotype is responsible for resistance of cancer cells to conventional cancer treatment [37, 38]. Our unpublished observation allowed us to hypothesize that molecules induced by gemcitabine treatment would render cancer cells resistant to the drug. Using cDNA microarray

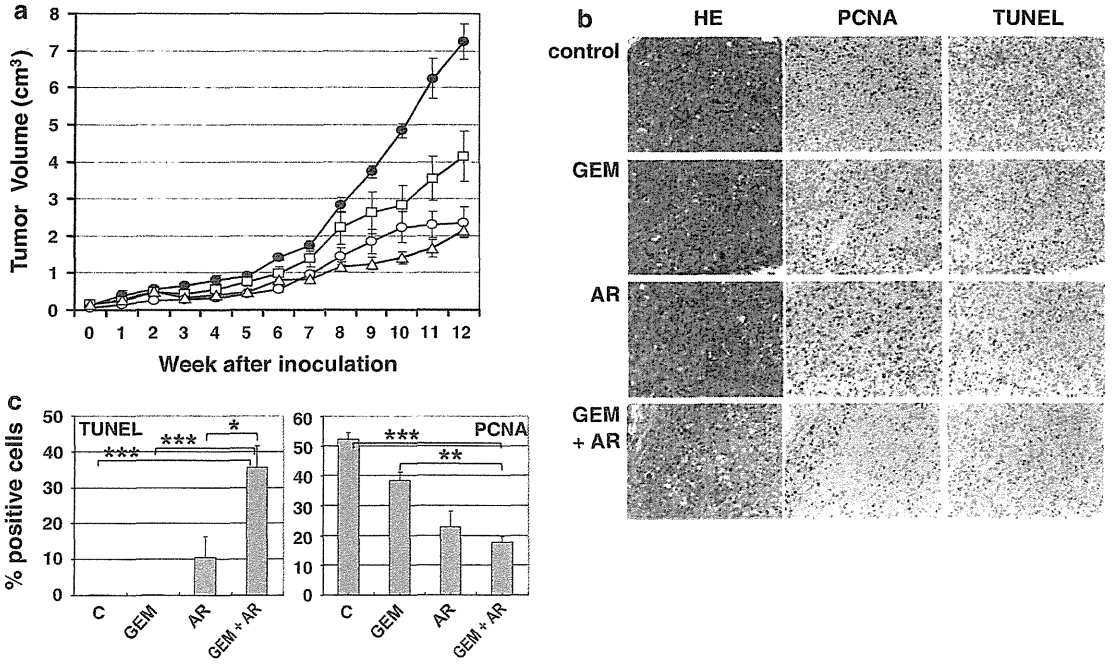

Fig. 6 Effect of gemcitabine, AR-A014418, and a combination of both agents against human pancreatic cancer cell xenografts in athymic mice, as detailed in Fig. 1a. **a** Time course of the effects of DMSO (*closed circle*), gemcitabine (20 mg/kg body weight; *open square*), AR-A014418 (2 mg/kg body weight; *open circle*), and a combination of the latter two agents (*open triangle*) on PANC-1 xenografts in mice. **b** Representative histological findings and frequency of PCNA- and TUNEL-positive tumor cells in the PANC-1 xenografts removed from mice at necropsy after 8-week treatment with the respective agents. **c** Relative number of PCNA- and TUNEL-positive tumor cells in PANC-1 xenografts removed from mice. Values are expressed as mean ± SDs. $*p < 0.05$, $**p < 0.01$, $***p < 0.001$ (the Mann–Whitney *U* test). **b**, **c** *C*, control; *GEM*, gemcitabine; *AR*, AR-A014418

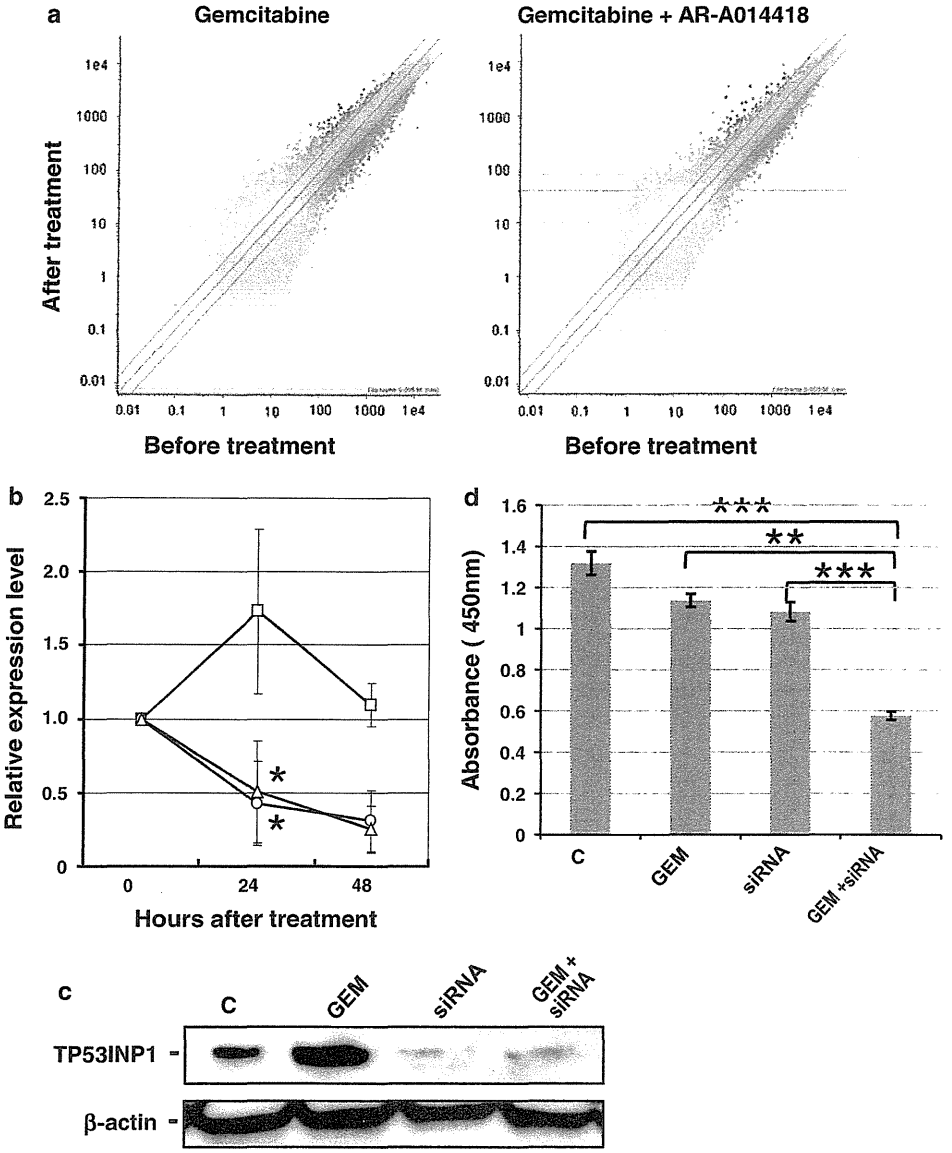

Fig. 7 **a** Changes in transcriptome profiles of PANC-1 cells treated with gemcitabine (190 μM) alone and in combination with AR-A014418 (10 μM) for 72 h. The scatter graphs were generated by the GeneSpring GX software package version 7.3.1. **b** Quantitative RT-PCR analysis of changes in TP53INP1 expression in PANC-1 cells treated with gemcitabine (190 μM; *open square*), AR-A014418 (10 μM; *open circle*), and the two agents in combination (*open triangle*) for 24 and 48 h. TP53INP1 expression levels in PANC-1 cells were normalized to levels in DMSO-treated cells at each time point. $*p < 0.05$. **c** Western blotting analysis of changes in TP35INP1 protein expression in PANC-1 cells treated with control (*C*; PBS and non-specific siRNA), gemcitabine (*GEM*), TP53INP1-specific siRNA (*siRNA*), and the two agents in combination (*GEM + siRNA*). β-actin expression was monitored as a loading control in each sample. **d** Effect of gemcitabine (50 mg/mL, 190 μM), TP53INP1-specific siRNA (10 nM), and the two agents in combination on PANC-1 cell survival. As a control, cells were treated with PBS and non-specific siRNA (10 nM). The relative number of viable cells after 48 h of treatment was measured by the WST-8 assay. Each assay was done in four wells three times. Data are presented as mean ± SD. *Asterisks* indicate statistically significant differences ($**p < 0.01$; $***p < 0.001$) between cells treated with control (*C*, PBS and non-specific siRNA), gemcitabine (*GEM*), TP53INP1-specific siRNA (*siRNA*), and the two agents in combination (*GEM + siRNA*)

analysis, we detected 84 genes that were significantly upregulated in PANC-1 cells by gemcitabine treatment and downregulated when treated in combination with a GSK3β inhibitor. Gene ontology analysis suggested involvement of these molecules in the pathways mediating cell cycle, cell proliferation, and cell death. We believe that some of them may participate in the mechanism by which GSK3β inhibition modifies PANC-1 cell sensitivity to gemcitabine.

Table 1 Representative gene expression changes in PANC-1 cells treated with gemcitabine and a GSK3β inhibitor

Group	GEM	GEM + AR	Number of genes
A	>4-fold	<1	84 genes
B	<1	>4	267 genes
C	1 < GEM < 4	>8	112 genes
			Total 463 genes
Top 10 molecules	**Fold change (GEM)**	**Fold change (GEM + AR)**	**Affymetrix ID**
Group A			
GDF11	4.058	0.0578	226234_at
FGD4	7.130	0.0649	230559_x_at
SLC1A4	4.257	0.1420	212810_s_at
FAM129A	5.767	0.1429	217967_s_at
APOBEC3F	4.734	0.1962	214995_s_at
SLFN13	4.465	0.2534	1558217_at
UCN	4.168	0.2518	206072_at
TP53INP1	5.959	0.2631	225912_at
HSPB11	4.311	0.2938	214163_at
C2ORF72	4.061	0.3067	213143_at
Group B			
MET	0.9747	44.209	213816_s_at
FNIP1	0.6262	36.832	1559060_a_at
ATP11B	0.3406	36.384	238811_at
ZNF33A	0.5910	26.291	224276_at
MED13	0.6793	25.170	244611_at
MAP4K5	0.7294	24.273	211081_s_at
TMEM87A	0.7342	24.100	223772_s_at
EIF1	0.8787	23.810	228967_at
RBM33	0.7305	20.929	1554096_a_at
BRAF	0.4713	19.362	240463_at
Group C			
APC	1.173	92.673	216933_x_at
ACDCP1	1.185	83.170	1554110_at
ATG7	1.094	48.946	1569827_at
MPHOSPH6	1.881	30.896	1554906_a_at
ZBTB11	1.326	29.302	230082_at
PMS1	1.749	26.298	1554742_at
ATOH7	2.123	25.071	1552879_a_at
HELLS	1.803	23.928	234040_at
OSBPL10	1.342	23.480	231656_x_at
MBNL	1.145	22.277	1558111_at

GEM gemcitabine, *AR* AR-A014418

Group A: GDF11, growth differentiation factor 11; FGD4, FYVE RhoGEF and PH domain containing 4; SLC1A4, solute carrier family 1 (glutamate/neutral amino acid transporter) member 4; FAM129A, family with sequence similarity 129 member A; APOBEC3F, apolipoprotein B mRNA editing enzyme catalytic polypeptide-like 3F; SLFN13, schlafen family member 13; UCN, urocortin; TP53INP1, tumor protein p53 inducible nuclear protein 1; HSPB11, heat shock protein family B (small) member 11; C2ORF72, chromosome 2 open reading frame 72

Group B: MET, met proto-oncogene (hepatocyte growth factor receptor); FNIP1, folliculin interacting protein 1; ATP11B, ATPase class VI type 11B; ZNF33A, zinc finger protein 33A; MED13, mediator complex subunit 13; MAP4K5, mitogen-activated protein kinase 5; TMEM87A, transmembrane protein 87A; EIF1, eukaryotic translation initiation factor 1; RBM33, RNA binding motif protein 33; BRAF, v-raf murine sarcoma viral oncogene homolog B1

Group C: APC, adenomatous polyposis coli; ACDCP1, cyclin M1; ATG7, autophagy related 7 homolog; MPHOSPH6, M-phase phosphoprotein 6; ZBTB11, zinc finger and BTB domain containing 11; PMS1, postmeiotic segregation increased 1; ATOH7, atonal homolog 7; HELLS, helicase lymphoid-specific; OSBPL10, oxysterol binding protein-like 10; MBNL, muscleblind-like

Among these molecules, we are interested in TP53INP1 because its expression is altered during the process in which pancreatic cancer cells acquire gemcitabine resistance [33]. RT-PCR and Western blotting analyses confirmed changes in its expression in PANC-1 cells treated with gemcitabine and a GSK3β inhibitor.

TP53INP1, also known as thymus-expressed acidic protein (TEAP), stress-induced protein (SIP), and p53-dependent damage-inducible nuclear protein 1 (p53DINP1), is a p53 target gene [39–41] that encodes the critical tumor suppressor in pancreatic carcinogenesis [33, 42]. DNA repair genes have an inhibitory effect on tumor development in the course of carcinogenesis. On the other hand, in our opinion, DNA repair genes may be protective for cancer cells against anticancer drugs after tumor development. TP53INP1 regulates p53-mediated apoptosis and cell cycle arrest in the G1 phase in response to cellular stresses. TP53INP1 expression is induced by various agents that cause cellular stress (adriamycin, cisplatin, ethanol, heat shock, oxidants, UV light) [39]. Gemcitabine treatment also causes cellular stress, and if cell cycle arrest occurs, the cell begins the process of repairing DNA damage induced by gemcitabine. Such a repair process might lead cancer cells to become resistant to gemcitabine. In this study, GSK3β inhibition decreased TP53INP1 expression, which may prevent DNA repair in response to gemcitabine and induce apoptosis in pancreatic cancer cells. Indeed, TP53INP1 knockout cells are very sensitive to gemcitabine (unpublished observation). The precise mechanism of decreased TP53INP1 mRNA expression by GSK3β inhibition needs to be studied further.

We previously showed that inhibition of GSK3β in gastrointestinal cancer and glioblastoma cells was associated with increased p53 and p21 expression in tumor cells with wild-type p53, and with decreased Rb phosphorylation and cyclin-dependent kinase 6 expression in tumor cells irrespective of p53 status [21, 22]. Rb is known to function as a tumor suppressor by inducing cell cycle arrest at the G1 phase and by inhibiting activity of the E2F transcription factor [43]. Transcriptional targets of E2F include ribonucleotide reductase (RR), thymidylate synthase (TS), and thymidine kinase (TK) [44]. RR plays a critical role in cell cycle progression to the S phase and its increased expression renders pancreatic cancer cells less sensitive to gemcitabine [45]. Therefore, inhibition of GSK3β may sensitize pancreatic cancer cells to gemcitabine via sequential modification of the Rb/E2F pathway. It was recently reported that TS, a target of E2F transcription and fluoropyrimidine-derived chemotherapeutic agents, is frequently activated in primary pancreatic cancer tissues [46]. This suggests that inhibition of GSK3β also sensitizes pancreatic cancer cells to fluoropyrimidines, such as 5-fluorouracil and S-1, which are prescribed for patients with advanced and/or recurrent pancreatic cancer.

Acknowledgments We thank Ms. Yoshie Yoshida for technical assistance. This work was supported in part by Grants-in-Aids for Scientific Research from the Japanese Ministry of Education, Science, Sports, Technology and Culture (to T.S., Y.M, T.M.) and the Ministry of Health, Labor and Welfare (to T.M.), by grants from the Kanazawa Medical University Research Foundation (S2006-10 to T.S.) and the Pancreas Research Foundation of Japan (to T.S.), by a Grant for Collaborative Research from Kanazawa Medical University (C2008-3 to Y.M., T.S., T.M.) and by a Project Research Grant from the High-Tech Research Center of Kanazawa Medical University (H2010-11 to Y.M.).

References

1. Jemal A, Siegel R, Ward E, Murray T, Xu J, Thun MJ. Cancer statistics, 2007. CA Cancer J Clin. 2007;57:43–66.
2. Parkin DM, Bray F, Ferlay J, Pisani P. Global cancer statistics, 2002. CA Cancer J Clin. 2005;55:74–108.
3. Okusaka T, Ito Y, Ueno H, Ikeda M, Takezako Y, Morizane C, et al. Phase II study of radiotherapy combined with gemcitabine for locally advanced pancreatic cancer. Br J Cancer. 2004;91:673–7.
4. Okusaka T, Kosuge T. Systemic chemotherapy for pancreatic cancer. Pancreas. 2004;28:301–4.
5. Li D, Xie K, Wolff R, Abbruzzese JL. Pancreatic cancer. Lancet. 2004;363:1049–57.
6. Schneider G, Siveke JT, Eckel F, Schmid RM. Pancreatic cancer: basic and clinical aspects. Gastroenterology. 2005;128:1606–25.
7. Burris HA III, Moore MJ, Andersen J, Green MR, Rothenberg ML, Modiano MR, et al. Improvements in survival and clinical benefit with gemcitabine as first-line therapy for patients with advanced pancreas cancer: a randomized trial. J Clin Oncol. 1997;15:2403–13.
8. Hruban RH, Goggins M, Parsons J, Kern SE. Progression model for pancreatic cancer. Clin Cancer Res. 2000;6:2969–72.
9. Bardeesy N, DePinho RA. Pancreatic cancer biology and genetics. Nat Rev Cancer. 2002;2:897–909.
10. Giroux V, Dagorn JC, Iovanna JL. A review of kinases implicated in pancreatic cancer. Pancreatology. 2009;9:738–54.
11. Moore MJ, Goldstein D, Hamm J, Figer A, Hecht JR, Gallinger S, et al. Erlotinib plus gemcitabine compared with gemcitabine alone in patients with advanced pancreatic cancer: a phase III trial of the National Cancer Institute of Canada Clinical Trials Group. J Clin Oncol. 2007;25:1960–6.
12. Furukawa T. Molecular targeting therapy for pancreatic cancer: current knowledge and perspectives from bench to bedside. J Gastroenterol. 2008;43:905–11.
13. Jope RS, Yuskaitis CJ, Beurel E. Glycogen synthase kinase-3 (GSK3): inflammation, diseases, and therapeutics. Neurochem Res. 2007;32:577–95.
14. Jope RS, Johnson GV. The glamour and gloom of glycogen synthase kinase-3. Trends Biochem Sci. 2004;29:95–102.
15. Doble BW, Woodgett JR. GSK-3: tricks of the trade for a multitasking kinase. J Cell Sci. 2003;116:1175–86.
16. Harwood AJ. Regulation of GSK-3: a cellular multiprocessor. Cell. 2001;105:821–4.
17. Cohen P, Goedert M. GSK3 inhibitors: development and therapeutic potential. Nat Rev Drug Discov. 2004;3:479–87.
18. Meijer L, Flajolet M, Greengard P. Pharmacological inhibitors of glycogen synthase kinase 3. Trends Pharmacol Sci. 2004;25:471–80.
19. Shakoori A, Ougolkov A, Yu ZW, Zhang B, Modarressi MH, Billadeau DD, et al. Deregulated GSK3β activity in colorectal

cancer: its association with tumor cell survival and proliferation. Biochem Biophys Res Commun. 2005;334:1365–73.
20. Shakoori A, Mai W, Miyashita K, Yasumoto K, Takahashi Y, Ooi A, et al. Inhibition of GSK-3β activity attenuates proliferation of human colon cancer cells in rodents. Cancer Sci. 2007;98: 1388–93.
21. Miyashita K, Kawakami K, Nakada M, Mai W, Shakoori A, Fujisawa H, et al. Potential therapeutic effect of glycogen synthase kinase 3β inhibition against human glioblastoma. Clin Cancer Res. 2009;15:887–97.
22. Mai W, Kawakami K, Shakoori A, Kyo S, Miyashita K, Yokoi K, et al. Deregulated GSK3β sustains gastrointestinal cancer cells survival by modulating human telomerase reverse transcriptase and telomerase. Clin Cancer Res. 2009;15:6810–9.
23. Miyashita K, Nakada M, Shakoori A, Ishigaki Y, Shimasaki T, Motoo Y, et al. An emerging strategy for cancer treatment targeting aberrant glycogen synthase kinase 3β. Anticancer Agents Med Chem. 2009;9:1114–22.
24. Hoeflich KP, Luo J, Rubie EA, Tsao MS, Jin O, Woodgett JR. Requirement for glycogen synthase kinase-3β in cell survival and NF-κB activation. Nature. 2000;406:86–90.
25. Schwabe RF, Brenner DA. Role of glycogen synthase kinase-3 in TNF-α-induced NF-κB activation and apoptosis in hepatocytes. Am J Physiol Gastrointest Liver Physiol. 2002;283:G204–11.
26. Ougolkov AV, Fernandez-Zapico ME, Savoy DN, Urrutia RA, Billadeau DD. Glycogen synthase kinase-3β participates in nuclear factor κB-mediated gene transcription and cell survival in pancreatic cancer cells. Cancer Res. 2005;65:2076–81.
27. Wilson W III, Baldwin AS. Maintenance of constitutive IκB kinase activity by glycogen synthase kinase-3α/β in pancreatic cancer. Cancer Res. 2008;68:8156–63.
28. Mamaghani S, Patel S, Hedley DW. Glycogen synthase kinase-3 inhibition disrupts nuclear factor-κB activity in pancreatic cancer, but fails to sensitize to gemcitabine chemotherapy. BMC Cancer. 2009;9:132.
29. Ougolkov A, Zhang B, Yamashita K, Bilim V, Mai M, Fuchs SY, et al. Associations among β-TrCP, an E3 ubiquitin ligase receptor, β-catenin, and NF-κB in colorectal cancer. J Natl Cancer Inst. 2004;96:1161–70.
30. Mai W, Miyashita K, Shakoori A, Zhang B, Yu ZW, Takahashi Y, et al. Detection of active fraction of glycogen synthase kinase 3β in cancer cells by nonradioisotopic in vitro kinase assay. Oncology. 2006;71:297–305.
31. Bhat R, Xue Y, Berg S, Hellberg S, Ormo M, Nilsson Y, et al. Structural insights and biological effects of glycogen synthase kinase 3-specific inhibitor AR-A014418. J Biol Chem. 2003;278:45937–45.
32. Steel GG, Peckham MJ. Exploitable mechanisms in combined radiotherapy-chemotherapy: the concept of additivity. Int J Radiat Oncol Biol Phys. 1979;5:85–91.
33. Jiang PH, Motoo Y, Sawabu N, Minamoto T. Effect of gemcitabine on the expression of apoptosis-related genes in human pancreatic cancer cells. World J Gastroenterol. 2006;12: 1597–602.
34. Holcomb B, Yip-Schneider M, Schmidt CM. The role of nuclear factor κB in pancreatic cancer and the clinical applications of targeted therapy. Pancreas. 2008;36:225–35.
35. Diamantidis M, Tsapournas G, Kountouras J, Zavos C. New aspects of regulatory signaling pathways and novel therapies in pancreatic cancer. Curr Mol Med. 2008;8:12–37.
36. Hamacher R, Schmid RM, Saur D, Schneider G. Apoptotic pathways in pancreatic ductal adenocarcinoma. Mol Cancer. 2008;7:64.
37. Wang Z, Li Y, Kong D, Banerjee S, Ahmad A, Azmi AS, et al. Acquisition of epithelial-mesenchymal transition phenotype of gemcitabine-resistant pancreatic cancer cells is linked with activation of the notch signaling pathway. Cancer Res. 2009;69: 2400–7.
38. Arumugam T, Ramachandran V, Fournier KF, Wang H, Marquis L, Abbruzzese JL, et al. Epithelial to mesenchymal transition contributes to drug resistance in pancreatic cancer. Cancer Res. 2009;69:5820–8.
39. Cano CE, Gommeaux J, Pietri S, Culcasi M, Garcia S, Seux M, et al. Tumor protein 53-induced nuclear protein 1 is a major mediator of p53 antioxidant function. Cancer Res. 2009;69: 219–26.
40. Tomasini R, Samir AA, Vaccaro MI, Pebusque MJ, Dagorn JC, Iovanna JL, et al. Molecular and functional characterization of the stress-induced protein (SIP) gene and its two transcripts generated by alternative splicing. SIP induced by stress and promotes cell death. J Biol Chem. 2001;276:44185–92.
41. Okamura S, Arakawa H, Tanaka T, Nakanishi H, Ng CC, Taya Y, et al. p53DINP1, a p53-inducible gene, regulates p53-dependent apoptosis. Mol Cell. 2001;8:85–94.
42. Gironella M, Seux M, Xie MJ, Cano C, Tomasini R, Gommeaux J, et al. Tumor protein 53-induced nuclear protein 1 expression is repressed by miR-155, and its restoration inhibits pancreatic tumor development. Proc Natl Acad Sci U S A. 2007;104: 16170–5.
43. Classon M, Harlow E. The retinoblastoma tumour suppressor in development and cancer. Nat Rev Cancer. 2002;2:910–7.
44. Ishida S, Huang E, Zuzan H, Spang R, Leone G, West M, et al. Role for E2F in control of both DNA replication and mitotic functions as revealed from DNA microarray analysis. Mol Cell Biol. 2001;21:4684–99.
45. Nakahira S, Nakamori S, Tsujie M, Takahashi Y, Okami J, Yoshioka S, et al. Involvement of ribonucleotide reductase M1 subunit overexpression in gemcitabine resistance of human pancreatic cancer. Int J Cancer. 2007;120:1355–63.
46. Nakahara O, Takamori H, Tanaka H, Sakamoto Y, Ikuta Y, Furuhashi S, et al. Clinical significance of dihydropyrimidine dehydrogenase and thymidylate synthase expression in patients with pancreatic cancer. Int J Clin Oncol. 2010;15:39–45.

Published OnlineFirst May 31, 2012; DOI:10.1158/0008-5472.CAN-12-0028

Therapeutics, Targets, and Chemical Biology

Cancer Research

Acyclic Retinoid Targets Platelet-Derived Growth Factor Signaling in the Prevention of Hepatic Fibrosis and Hepatocellular Carcinoma Development

Hikari Okada[1], Masao Honda[1,2], Jean S. Campbell[4], Yoshio Sakai[1], Taro Yamashita[1], Yuuki Takebuchi[1], Kazuhiro Hada[1], Takayoshi Shirasaki[1], Riuta Takabatake[1], Mikiko Nakamura[1], Hajime Sunagozaka[1], Takuji Tanaka[3], Nelson Fausto[4], and Shuichi Kaneko[1]

Abstract

Hepatocellular carcinoma (HCC) often develops in association with liver cirrhosis, and its high recurrence rate leads to poor patient prognosis. Although recent evidence suggests that peretinoin, a member of the acyclic retinoid family, may be an effective chemopreventive drug for HCC, published data about its effects on hepatic mesenchymal cells, such as stellate cells and endothelial cells, remain limited. Using a mouse model in which platelet-derived growth factor (PDGF)-C is overexpressed (*Pdgf-c Tg*), resulting in hepatic fibrosis, steatosis, and eventually, HCC development, we show that peretinoin significantly represses the development of hepatic fibrosis and tumors. Peretinoin inhibited the signaling pathways of fibrogenesis, angiogenesis, and Wnt/β-catenin in *Pdgf-c* transgenic mice. *In vitro*, peretinoin repressed the expression of PDGF receptors α/β in primary mouse hepatic stellate cells (HSC), hepatoma cells, fibroblasts, and endothelial cells. Peretinoin also inhibited PDGF-C–activated transformation of HSCs into myofibroblasts. Together, our findings show that PDGF signaling is a target of peretinoin in preventing the development of hepatic fibrosis and HCC. *Cancer Res; 72(17); 4459–71. ©2012 AACR.*

Introduction

Hepatocellular carcinoma (HCC) is one of the most common malignancies worldwide with a particularly poor patient outcome (1). It often develops as a result of chronic liver disease associated with hepatitis B or hepatitis C virus infection or with other etiologies such as long-term alcohol abuse, autoimmunity, and hemochromatosis (2–5). Despite the recent advances in antiviral therapy for hepatitis B or hepatitis C virus, these are insufficient to completely prevent the occurrence of HCC. Moreover, the recent increase in nonalcoholic fatty liver disease (NAFLD) associated with metabolic syndrome is a potential high-risk factor for the development of HCC (6).

HCC often develops during the advanced stages of liver fibrosis and is associated with deposits of extracellular matrix synthesized by activated stellate cells. During the course of chronic hepatitis, nonparenchymal cells, including Kupffer, endothelial, and activated stellate cells, release a variety of cytokines and growth factors. One of these growth factors is platelet-derived growth factor (PDGF), which is involved in fibrogenesis, angiogenesis, and tumorigenesis (7, 8). PDGF expression has been shown to be upregulated from the early stages of chronic hepatitis, suggesting its association with the development of fibrosis in chronic hepatitis C (CH-C; refs. 9 and 10). Overexpression of PDGF-C in mouse liver resulted in the progression of hepatic fibrosis, steatosis, and the development of HCC; this mouse model closely resembles the human HCC, which is frequently associated with hepatic fibrosis (7).

Peretinoin (generic name; code, NIK-333), developed by the Kowa Company, is an oral acyclic retinoid with a vitamin A–like structure, which targets the retinoid nuclear receptor. Oral administration of peretinoin was shown to significantly reduce the incidence of posttherapeutic HCC recurrence and improve the survival rates of patients in a clinical trial (11, 12). A large-scale clinical study including various countries is now planned to confirm its clinical efficacy.

Although peretinoin treatment can suppress HCC-derived cell line growth and inhibit experimental mouse or rat liver carcinogenesis (13, 14), the detailed mechanism of its effect has not been fully elucidated. Peretinoin has a high binding affinity to cellular retinoic acid-binding protein (15) and may interact with retinoic acid receptor-β and retinoid X receptor-α (16); however, the precise molecular targets for preventing HCC recurrence have not yet been elucidated.

Authors' Affiliations: [1]Department of Gastroenterology, Kanazawa University Graduate School of Medicine; [2]Department of Advanced Medical Technology, Kanazawa University Graduate School of Health Medicine; [3]Department of Oncologic Pathology, Kanazawa Medical University, Kanazawa, Japan; and [4]Department of Pathology, University of Washington School of Medicine, Seattle, Washington

Note: Supplementary data for this article are available at Cancer Research Online (http://cancerres.aacrjournals.org/).

Corresponding Author: Masao Honda, Department of Gastroenterology, Graduate School of Medicine, Kanazawa University, Takara-Machi 13-1, Kanazawa 920-8641, Japan. Phone: 81-76-265-2235; Fax: 81-76-234-4250; E-mail: mhonda@m-kanazawa.jp

doi: 10.1158/0008-5472.CAN-12-0028

Published OnlineFirst May 31, 2012; DOI:10.1158/0008-5472.CAN-12-0028

In this study, we used PDGF-C transgenic (*Pdgf-c* Tg) mice to show that PDGF-C signaling is a possible target of peretinoin in the prevention of hepatic fibrosis, angiogenesis, and the development of HCC.

Materials and Methods

Chemicals

The acyclic retinoid peretinoin (generic name; code, NIK-333) [(2E,4E,6E,10E)-3,7,11,15-tetramethyl-2,4,6,10,14-hexadecapentaenoic acid, C20H30O2, molecular weight 302.46 g/mol] was supplied by Kowa Company.

Animal studies

The generation and characterization of *Pdgf-c Tg* have been described previously (7). Wild-type and *Pdgf-c Tg* mice on a C57BL/6J background were maintained in a pathogen-free animal facility under a standard 12-hour/12-hour light/dark cycle. After weaning at week 4, male mice were randomly divided into the following 3 groups: (1) *Pdgf-c Tg* or wild-type (WT) mice given a basal diet (CRF-1, Charles River Laboratories Japan), (2) *Pdgf-c Tg* or WT mice given a 0.03% peretinoin-containing diet, (3) *Pdgf-c Tg* or WT mice given a 0.06% peretinoin-containing diet. Control mice were normal male homozygotes. At week 20, mice were sacrificed to analyze the progression of hepatic fibrosis ($n = 15$ for each of the 3 groups). At week 48, mice were sacrificed to analyze the development of hepatic tumors ($n = 31$ for the basal diet group, $n = 37$ for the 0.03% peretinoin group, and $n = 17$ for the 0.06% peretinoin group). The incidence of hepatic tumors, maximum tumor size, and liver weight were evaluated. None of the treated WT mice given a diet of 0.03% peretinoin died, but death occurred in 5% of WT mice around after 36 weeks of age receiving a 0.06% peretinoin diet, probably because of its toxicity. In *Pdgf-c Tg* mice, death was observed at similar frequency as WT mice that received 0.06% peretinoin diet.

All animal experiments were carried out in accordance with Guidelines for the Care and Use of Laboratory Animals at the Takara-Machi Campus of Kanazawa University, Japan.

Cell culture

Human HCC cell lines Huh-7, HepG2, and HLE, the mouse fibroblast cell line NIH3T3, human umbilical vein endothelial cells (HUVEC), and human stellate cells Lx-2 (kindly provided by Dr. Scott Friedman, Mount Sinai School of Medicine, New York, NY) were maintained in Dulbecco's Modified Eagle Medium (DMEM; Gibco) supplemented with 10% FBS (Gibco), 1% L-glutamine (Gibco), and 1% penicillin/streptomycin (Gibco) in a humidified atmosphere of 5% CO_2 at 37°C. 1 to 5×10^4 cells were seeded in each well of a 12-well plate the day before serum starvation in serum-free DMEM for 8 hours. The culture medium was then replaced with serum-free medium containing peretinoin. After 24-hour incubation, cells were harvested for analysis.

Isolation and culture of mouse hepatic stellate cells

Hepatic stellate cells (HSC) were isolated from C57BL/6J mice and the effect of recombinant human PDGF-C and peretinoin on HSCs was evaluated *in vitro*. Pronase-collagenase liver digestion was used to isolate HSC from wild-type mice. All experiments were replicated at least twice. Freshly isolated HSCs suspended in culture medium were seeded in uncoated 24-well plates and incubated at 37°C in a humidified atmosphere of 5% CO_2 for 72 hours. Nonadherent cells were removed with a pipette and the culture medium was replaced with medium containing 80 ng/mL recombinant human PDGF-C (Abnova) with or without peretinoin or 9-*cis*-retinoic acid (9cRA; 5 or 10 μmol/L). Cells were harvested for analysis after 24-hour incubation.

Isolation of peripheral blood mononuclear cells

Peripheral blood mononuclear cells were harvested and labeled with FITC-conjugate CD34 (Cell Lab) and R-Phycoerythrin (PE)-conjugated CD31 antibodies (Cell Lab) for 30 minutes at 4°C. After washing with 1 mL PBS, CD31 and CD34 surface expression was measured with a FACSCalibur flow cytometer (BD Biosciences). All flow cytometric data were analyzed using FlowJo software (Tree Star).

Gene expression profiling

Gene expression profiling in mouse liver was evaluated using the GeneChip Mouse Genome 430 2.0 Array (Affymetrix). Liver tissue from WT, *Pdgf-c Tg*, and *Pdgf-c Tg* with 0.06% peretinoin mice all at weeks 20 and 48 was obtained and a total of 34 chip assays were conducted as described previously (17). Expression data have been deposited in the Gene Expression Omnibus (GEO; NCBI Accession; GSE31431).

Pathway analysis was conducted using MetaCore (GeneGo). Functional ontology enrichment analysis was conducted to compare the Gene Ontology (GO) process distribution of differentially expressed genes ($P < 0.01$; refs. 10 and 17). Direct interactions among differentially expressed genes between *Pdgf-c Tg* mice with or without peretinoin administration were examined as reported previously (10). Each connection represents a direct, experimentally confirmed, physical interaction (MetaCore).

Histopathology and immunohistochemical staining

Mouse liver tissues were fixed in 10% formalin and stained with hematoxylin and eosin. The liver neoplasms (HCC and liver cell adenoma) were diagnosed according to previously described criteria (18, 19). Hepatic fibrosis was evaluated by Azan staining. Percentages of fibrous areas were calculated microscopically using an image analysis system (BIOREVO BZ-9000: KEYENCE Japan). Immunohistochemical (IHC) staining was conducted by an immunoperoxidase technique with an Envision kit (DAKO). Primary antibodies used were: rabbit polyclonal PDGFR-α (1:100 dilution), PDGFR-β (1:100 dilution), VEGFR1 (1:100 dilution), desmin (1:100 dilution), β-catenin (1:200 dilution), and mouse monoclonal cyclin D1 (1:400 dilution; all from Cell Signaling Technology); collagen 1 (1:100 dilution), collagen 4 (1:100 dilution), CD31 (1:100 dilution), and CD34 (1:100 dilution; all from Abcam, Cambridge, MA); and Tie-2 (1:80 dilution) and Myc (1:100 dilution; both from Santa Cruz Biotechnology).